

**EFFECTS OF TEMPERATURE AND FATTY ACID
COMPOSITION ON THE KINEMATIC VISCOSITY OF
BIODIESEL: EMPIRICAL AND MATHEMATICAL
MODELS**

**A THESIS SUBMITTED TO THE GRADUATE
SCHOOL OF APPLIED SCIENCES
OF
NEAR EAST UNIVERSITY**

**By
GIDION ANYONG ATIM**

**In Partial Fulfillment of the Requirements for
The Degree of Master of Science
in
Mechanical Engineering**

NICOSIA, 2017

**GIDION ANYONG
ATIM**

**EFFECTS OF TEMPERATURE AND FATTY ACID
COMPOSITION ON THE KINEMATIC VISCOSITY OF
BIODIESEL: EMPIRICAL AND MATHEMATICAL MODELS**

**NEU
2017**

**EFFECTS OF TEMPERATURE AND FATTY ACID
COMPOSITION ON THE KINEMATIC VISCOSITY OF
BIODIESEL: EMPIRICAL AND MATHEMATICAL
MODELS**

**A THESIS SUBMITTED TO THE GRADUATE
SCHOOL OF APPLIED SCIENCES
OF
NEAR EAST UNIVERSITY**

**By
GIDION ANYONG ATIM**

**In Partial Fulfillment of the Requirements for
The Degree of Master of Science
in
Mechanical Engineering**

NICOSIA, 2017

**Atim Gidion ANYONG: EFFECTS OF TEMPERATURE AND FATTY ACID
COMPOSITION ON THE KINEMATIC VISCOSITY OF BIODIESEL: EMPIRICAL
AND MATHEMATICAL MODELS**

**Approval of Director of Graduate School of
Applied Sciences**

Prof. Dr. Nadire ÇAVUŞ

**We certify this thesis is satisfactory for the award of the degree of Master of Science in
Mechanical Engineering**

Examining Committee in Charge:

Prof. Dr. Adil AMİRJANOV

Committee Chairman, Department of
Computer Engineering, NEU

Dr. Youssef KASSEM

Department of Mechanical Engineering
NEU

Assist. Prof. Dr. Hüseyin ÇAMUR

Supervisor, Mechanical Engineering
Department, NEU

I hereby declare that, all the information in this document has been obtained and presented in accordance with academic rules and ethical conduct. I also declare that, as required by these rules and conduct, I have fully cited and referenced all materials and results that are not original to this work.

Name, Last Name:

Signature:

Date:

ACKNOWLEDGEMENTS

This thesis wouldn't have been possible without the patience of my principal supervisor, Assist. Prof. Dr. Hüseyin ÇAMUR. I am very thankful and indebted to Dr. Youssef KASSEM, for constant guidance and encouragement. To the crew of lecturers at the NEU Engineering department, I say great thanks. My gratitude to some of my course mates, who collaborated with me, especially during periods of group assignments and Examination. Their directives were never in any way minimal to my success at NEU

My unlimited thanks and heartfelt love is dedicated to my wife, children, my Dad, Mum, brothers, sisters and the rest of my.

I also wish to thank my special friends, Mr. Bornu Nornubari Barituka and Mr. Asuelimen O. Theophilus for all the knowledge they taught me in computer. Their ideas towards my success are unlimited

Thank you Mr. Muna Louis, Mr. Teke Levis and Mr. Abong Joel for your care and collaboration

Thank you God almighty for the strength to realize this work.

To my wife and children...

ABSTRACT

The dwindling of fossil fuel sources the world over has triggered engineers to develop alternative energy sources such as biodiesel. Kinematic viscosity is one of the most indispensable properties of biodiesel fuels, with a greater influence in the injection system of engines. This work is destined to contrast the predicting abilities of the Response Surface methodology, Adaptive Neuro-Fuzzy Inference System (ANFIS) and a Mathematical Correlation Model, to envisage the kinematic viscosity of fatty acid methyl esters (FAMES) biodiesel. The database for these models was gathered from the review of literature. For simplicity and the quest for accurate results, the data was separated into saturated and unsaturated FAMES. Temperature, number of carbon atoms, number of hydrogen atoms were the input parameters used for the various models. This work embraces empirical models, considering their transformative impact in the development of several modeling in the field of engineering. The developed models produced pragmatic results; however the ANFIS model was more precise, followed by the RSM, in predicting kinematic viscosity results.

Keywords: ANFIS; Biodiesel; FAME; Model; Kinematic Viscosity; RSM

ÖZET

Dünyayı küçülen fosil yakıt kaynakları, mühendisleri biyodizel gibi alternatif enerji kaynakları geliştirmeye yönlendirdi. Kinematik viskozite, biyodizel yakıtlarının vazgeçilmez özelliklerinden biridir ve motorların enjeksiyon sisteminde daha büyük bir etkiye sahiptir. Bu çalışma, yağ asidi metil esterlerinin (FAMEs) biyodizelin kinematik viskozitesini öngörmek için Tepki Yüzeyi metodolojisinin, Uyarlamalı Sinirsel Bulanık Çıkarım Sistemi (ANFIS) ve Matematiksel Bir Korelasyon Modeli'nin öngörme yeteneklerinin karşıtlığı için tasarlanmıştır. Bu modeller için veri tabanı literatür taramasından derlenmiştir. Sıcaklık, karbon atomu sayısı, hidrojen atomları sayısı, çeşitli modeller için kullanılan girdi parametreleridir. Geliştirilen modeller pragmatik sonuçlar üretti; Bununla birlikte, ANFIS modeli, kinematik viskozite sonuçlarının tahmininde daha kesinti.

Anahtar Kelimeler: ANFIS; Biyodizel; RSM; Kinematik Viskozite; model

TABLE OF CONTENTS

ACKNOWLEDGEMENTS	ii
ABSTRACT	v
ÖZET	vi
TABLE OF CONTENTS	vii
LIST OF TABLES	x
LIST OF FIGURES	Xi
LIST OF SYMBOLS USED	Xiii
LIST OF ABBREVIATIONS	Xiv
 CHAPTER 1: INTRODUCTION	
1.1 Background.....	1
1.2 Literature Review.....	2
1.3 Research Aims.....	6
1.4 Thesis Outline.....	7
 CHAPTER 2: BIODIESEL	
2.1 Definition.....	8
2.2 Some Major Advantages of Biodiesel.....	8
2.3 Disadvantages of Biodiesel.....	10
2.4 The Concept of Viscosity.....	11
2.5 Dynamic Viscosity.....	13
2.6 Kinematic Viscosity.....	15
2.7 Factors Affecting Fluid Viscosity.....	15
 CHAPTER 3: THEORIES	
3.1 Fuzzy Logic Based Algorithms.....	17
3.2 Analysis with Fuzzy Inference System.....	17
3.3 Types of Fuzzy System.....	18

3.4 Adaptive Network Based Fuzzy Inference System.....	18
3.5 Adaptive Neuro-Fuzzy Inference System (ANFIS).....	19
3.6 Response Surface Methodology.....	22
3.7 Mathematical Correlation.....	23

CHAPTER 4: METHODOLOGY

4.1 The Experiment Database.....	25
4.2 Empirical Model.....	31

CHAPTER 5: RESULTS AND DISCUSSIONS

5.1 Methods of Application of ANFIS for Prediction of FAME's Kinematic Viscosity...	33
5.2 Modeling the Kinematic Viscosity of FAME Biodiesel.....	
5.3 Method of Application of ANFIS for the Prediction of kinematic Viscosity of Unsaturated Fatty Acid Methyl Esters.....	
5.4 Modeling of Kinematic Viscosity of Unsaturated FAMES, using ANFIS.....	51
5.5 Response Surface Methodology for Kinematic Viscosity of Saturated FAMES.....	55
5.6 Response Surface Methodology for Kinematic Viscosity of Unsaturated FAMES....	62
5.7 Summary of the Response Surface Methodology Results (RSM)	68
5.8 Mathematical Model.....	69
5.9 Comparing the Correlation Models for FAMES Biodiesel.....	73

CHAPTER 6: CONCLUSION 74

REFERENCES	76
-------------------------	----

LIST OF TABLES

Table 4.1: Sources of Data from Literature	26
Review.....	
Table 4.2: Kinematic Viscosity of Unsaturated FAMES at Different	26
Temperatures.....	
Table 4.3: Kinematic Viscosity of Saturated FAMES	28
Data.....	
Table 4.4: Names and Formulae of Various	31
FAMES.....	
Table 4.5: Limits of the input and Output Parameters for the	32
Models.....	
Table 5.1: The ANFIS Information by the Hybrid Optimum	34
Model.....	
Table 5.2: The ANFIS Information by the Back-propagation Optimum Method	35
.....	
Table 5.3: System Parameter of the ANFIS	36
Model.....	
Table 5.4: Predicting Error for Saturated	36
FAMES.....	
Table 5.5: Comparing Experimental and ANFIS Results for Saturated	39
FAMES.....	
Table 5.6: The ANFIS Information by the Hybrid Optimum	46
Model.....	
Table 5.7: ANFIS Information by the Back-propagation Optimum	47
Model.....	
Table 5.8: System Parameter of the ANFIS	48
model.....	
Table 5.9: ANFIS Testing Error to predict the Kinematic Viscosity of Saturated	48
FAMES.....	

.....	
Table 5.10: Comparative Study of Experimental and ANFIS results for Unsaturated	52
FAMEs.....	
Table 5.11: RSM Results for Saturated and Unsaturated	68
FAMEs.....	
Table 5.12: Mathematical Model Results for Saturated	69
FAMEs.....	
Table 5.13: Mathematical Model Results for Saturated	71
FAMEs.....	
Table 5.14: R^2 Values for the Various Models	73
.....	

LIST OF FIGURES

Figure 2.1:	Fluid flow between two parallel plates	13
Figure 2.2:	Illustration of viscous force differential expression	14
Figure 3.1:	Basic ANFIS architecture	19
Figure 3.2:	A Flowchart of hybrid learning procedure of ANFIS	21
Figure 5.1:	ANFIS architecture for kinematic viscosity of FAMES biodies	33
Figure 5.2:	Rule viewer of ANFIS model for Saturated FAME biodiesel	37
Figure 5.3:	Surface viewer of ANFIS model for saturated FAME biodiesel	37
Figure 5.4:	Plot of experimental data versus ANFIS predicted data for Saturated FAME.....	38
Figure 5.5:	ANFIS architecture for predicting the kinematic viscosity of unsaturated FAME biodiesel.....	39
Figure 5.6:	Rule viewer of ANFIS model for the kinematic viscosity of unsaturated fatty acid methyl biodiesel	49
Figure 5.7:	Surface viewer of ANFIS model for kinematic viscosity of unsaturated FAMES.....	50
Figure 5.8:	Plot of experimental values versus ANFIS values for unsaturated kinematic viscosity of FAME.....	51
Figure 5.9:	Contour plot for saturated kinematic viscosity, using RSM prediction model, with NC as parameter	56
Figure 5.10:	Contour plot of kinematic viscosity for saturated with NH, as parameter.....	57
Figure 5.11:	Surface plot of viscosity versus temperature and number of carbon atoms.....	58
Figure 5.12:	Surface plot structure for viscosity versus temperature and number of hydrogen atom.....	59
Figure 5.13:	Plot of residual values versus fitted values, for saturated FAME	60
Figure 5.14:	Plots of viscosity with a single parameter	61

Figure 5.15: Contour plot for viscosity versus T, NC, for unsaturated FAME.....	63
Figure 5.16: Contour plot for viscosity versus T, NH for unsaturated FAME.....	64
Figure 5.17: Surface plot for viscosity versus T, NC, for unsaturated FAME	65
Figure 5.18: Contour plot of viscosity versus T, NH for unsaturated FAME	66
Figure 5.19: Plots of viscosity versus single variable, for unsaturated FAME	66
Figure 5.20: Viscosity changes with different parameter plots, for unsaturated	67
Figure 5.21: Plot of residual versus fitted values	67
Figure 5.22: Fitting of predicted kinematic viscosity values for saturated FAME, and experimental values.....	70
Figure 5.23: Fitting of predicted kinematic viscosity values of unsaturated FAME, with experimental values, for the mathematical model.....	72

LIST OF ABBREVIATIONS

AAD:	Absolute Average Deviation
ANFIS:	Adaptive Neuro Fuzzy Inference System
ASTM:	American Society for Testing Materials
B20:	20 Percent Biodiesel, 80 Percent Petroleum Diesel
B100:	100 Percent Biodiesel
EXP:	Experiment
FAME:	Fatty Acid Methyl Ester Biodiesel
FIS:	Fuzzy Inference System
LTVR:	Low Temperature Viscosity Ratio
NC:	Number of Carbon Atoms
NH:	Number of Hydrogen Atoms
RSM:	Response Surface Methodology

LIST OF SYMBOLS USED

E	Backward propagation of errors
I	Node
M	Molecular weight (g/mol.)
n	Node number
O	Output layer
T	Temperature (K)
u	Velocity (m/s)
x_i	Input data

Greek Symbols

μ	Dynamic viscosity	(N.s/m ²)
ν	Kinematic viscosity	(mm ² /s)
ρ	Density	(kg/m ³)
τ	Shear Stress	(N/m ²)

CHAPTER 1

INTRODUCTION

1.1 Background

The applications of petroleum diesel in engines the world over has been a major problem, due to the rigorous emission law, the dwindling of fossil fuels, the interrelation of fossil fuels with politics and the huge sums of money levied on importation by some countries. Fossil fuels contribute 80% of the primary energy consumed in the world, with the transport sector swamping 58% of it (Canon and Fenske, 1938). These have triggered engineers to seek an alternative engine fuel known as biodiesel (Meher et al., 2006).

Biodiesel is a sparkling burning, environmental friendly, renewable fuel made using either of the following; vegetable oil, animal fats, discarded cooking gas, and a rendered form of beef or mutton fat called tallow. Biodiesel is made via a chemical process which converts oils and fats of natural origin into fatty acids methyl esters (FAMES), known as trans-etherification. Because of its reduced emission of toxic gases, its biodegradability, its affordability, and availability, biodiesel is increasingly being applied in engines and automobiles across the world. It is an exceedingly sustainable energy source, governed by ASTM D6751 quality parameter (Pratas et al., 2010). Notably the application of biodiesel in engines assures high lubricity and is associated with longer engine span. One of the fundamental properties of biodiesel is its viscosity. The viscosity of biodiesel is its resistance to flow. Engineers give attention and consideration to biodiesel's greater viscosity, as likened to petroleum fuel diesel. This due to the extra injection pressure experienced during engine warm-up (Meher et al., 2006).

Because of its paramount effects on engine performance, viscosity is considered a substantial property of biodiesel. The higher value of viscosity has a unique advantage of promoting fuel spray penetration into the combustion chamber. However, a lot of unpropitious effects are associated to the higher value of viscosity. That is, fuel injection pressure is unrestrained causing deficient fuel spray and consequently an incomplete

combustion process; amid others (Ramirez, 2013). A firm knowledge about this high value of viscosity and the interrelation of viscosity and temperature is imperative. The viscosity of biodiesel fuel is affected by the composition of fatty acid in it. Fatty acid composition of oils and fats are feedstock dependent and are affected by the type of soil, health of the plants and the maturity of the plants at harvest (Manning and Canon, 1960). As a consequence, the fatty acid composition of biodiesel fluctuates from one area to the other, alongside those produced from the same plant or animal species. This is a major impediment to biodiesel fuel (Canon and Fenske, 1938).

The density of any substance is its mass per unit volume. It is also an important physical property of biodiesel. The concept of density in biodiesel application allows an accurate measurement of the exact fuel quantity that can supply an effective combustion. The high pressure pump and injectors form the injector system, which allows a discrete volume of fuel to enter the fuel cylinder. This volume of fuel is calculated by the vehicle's electronic control unit (Lapeurta et al., 2010). Principally the density of a fuel influences the distribution of equivalent fuel proportion in the injector system and the fuel spray momentum. Accurate data for density values promotes engineering works such as; the designing of storage tanks, reactors, distillation units and pipes (Pratas et al., 2011). The density of fatty acids biodiesel depends on the raw materials used to produce the biodiesel and the alkyl esters profile in it (Pratas et al., 2011).

1.2 Literature Review

Few methods have been developed to predict the density and kinematic viscosity of FAMES biodiesel; however a lot of methods are in existence for the density and viscosity of petroleum fuels, with dependency on temperature. The impediment of these methods for biodiesel is that there are limited to envisage the above properties at two temperatures, exemplarily 288.15K for density and 313.15K for kinematic viscosity. These limitations are guided by several bodies, stipulating the standards for biodiesel. These include the American ASTM D6751 and the European CEN EN 14214 (Pratas et al., 2010).

Juan C. et al (2013), in their work titled; predicting the kinematic viscosity of FAMEs and biodiesel: Empirical models, developed three complementary models. Their models were applicable to a wide range of temperature and hydrocarbon length. Their average and maximum deviations for saturated FAMEs were 1.33 and 4.01% respectively. At the same time, their second model computed the average and maximum deviations for saturated FAMEs as 2.88 and 9.34% respectively (Juan et al., 2013)

Maria et al. (2010), in their paper titled; Density and viscosities of fatty acid methyl esters, developed a reliable model from the data, at a temperature range of 273.13K to 363.15K. Their results presented a less than 0.15% for density and less than 5% for viscosity, as deviations. They further went ahead to evaluate three productive models with the density and kinematic viscosity data used in their model. In their finding, the GCVOL group contribution method was shown to produce densities within 1% deviation Maria et al. (2010). The method of Cerianic and Meirlles (CM) and of Marreiro and Gani were equally applied to viscosity data. The first of their three methods provided a rational description of fatty acids and esters. Suriga et al. (2014) worked on “An empirical equation for estimation of kinematic viscosity of fatty acids methyl esters and biodiesel”. At a temperature range of 20⁰C -100⁰C and at atmospheric pressure, they estimated the kinematic viscosity of biodiesel. Their result gave an absolute average deviation (AAD), of 4.155% for saturated FAMEs, 3.25% for unsaturated FAMEs, 6.95% for biodiesel and 2.9% for biodiesel blends. This model was long-established excellent to estimate the viscosity of biodiesel that has customary fatty acids (Suriya et al. 2015)

Gerhard et al. (2000) worked on the kinematic viscosity of biodiesel components (fatty acids alkyl esters) and related compounds at low temperature, aimed at creating data to develop biodiesel fuel optimization from the composition of fatty acids ester. Low temperature viscosity ratio (LTVR), with data from 0⁰C to 40⁰C was applied in the appraisal of specific compounds. Species of saturated, mono-saturated, di-unsaturated, and tri-unsaturated fatty esters and methyl ricinoleate were examined.

They envisage that the OH group in the methyl ricinoleate, triolein, some fatty alcohols and some alkanes led to a substantial increase in the viscosity. The highest value of viscosity was measured from compound of Oleic acid, amongst all the biodiesel compounds that are liquids at low temperatures (Gerald and Kelvin (2014)

Out with a comprehensive evaluation of the density of neat fatty acid. They selected biodiesel as a function of methyl, ethyl, propyl and butyl esters, in addition to triacylglycerol that range from C8:0 – C22:0. A temperature range of 15⁰C-40⁰C was applied. After a careful analysis of the data, their result showed that the density decreases, as the chain length and saturation of the fatty acid compounds increases. However, they sorted that *trans*-fatty acid compounds divulge lower density whereas the contrary happens for *cis* -fatty compounds. Gerhard et al extended their findings, by reporting density data for saturated odd numbered compounds, stretching to poly-unsaturated fatty esters like; C18:0, C20:0 and C22:0 (Gerald and Kelvin, 2014).

K.Y. Liew et al. (2000) predicted the viscosities and densities of methyl esters of n-Alkanoic acids. The methyl esters chosen were hexanoic acid, heptanoic acid, octanoic acid, decanoic and dodecanoic acids. Experimental data for a temperature range of 10⁰C - 80⁰C, at 5⁰C interval was selected. They established that, densities of methyl esters make a linear variation with temperature. They equally plotted fluidities of esters versus molar volumes and realized smooth curves. A modified equation connecting fluidity and temperature was formulated. Expectedly, all their calculated results agreed with experimented results.

Within contemporary time, Ramirez (2000) anticipated a four parameter amendable empirical model to predict the dynamic viscosity of FAMES. He computed the viscosity in relation to the molecular weight, number of double bonds, and temperature, with unsaturated FAMES. At the completion of his work, significant deviations were noticed between calculated and experimental viscosities. He came out with a minimum deviation of 0.09%, maximum deviation of 29.63% and an average absolute deviation of 6.04%. In all, a total of 296 data points were used. An over-all AAD of 6.36 was experienced.

The work done by Baroutian et al. and Veny et al. saw the application of Janarthanan's empirical method, together with the Spencer and Danner model, to predict the Jatropha and Palm biodiesel densities at various temperatures, yielded accurate results.

Additionally, Anand et al. (2010) proposed a model based on the modified Racket equation that predicted the density of thirteen biodiesel samples from vegetable oils, at 288.15K.

Likewise, Pratas et al. (2011) proposed a method that depended on the Kay's mixing rule and the group contribution method for producing the density of 10 biodiesel samples at various temperatures.

Yuan et al. (2000) used the Vogel equation to correlate the viscosity of some biodiesel samples with temperature.

Do Carmo et al. (2012) compared five models. These included the Yuan, reversed Yuan, one-fluid and two-fluid. He predicted viscosity as a function of temperature, for thirty pure biodiesel samples and four biodiesel blends.

Because of the significance of an accurate and reliable model, this work seeks to develop improved empirical models to predict the kinematic viscosity of fatty acids biodiesel, as a function of temperature. As a means to overcome this great challenge, three interpolative models are engaged. ANFIS (the Adaptive Neural Inference System), the Response Surface Methodology, and a Mathematical Model are applied. Results from these three models are compared, to select the best model that can be used to congregate viscosity data for future applications in engines. Such a method shall be determined from the rate of deviation it produces.

Several mathematical models have been used to calculate the kinematic viscosity of fatty acid methyl biodiesel. Luis Felipe (2012) modeled empirical correlations for the prediction of the density and dynamic viscosity of FAME biodiesel. In all 19 FAMEs biodiesel were used with 351 experimental data. His mathematical models are shown in the following equations.

$$\rho = A + \frac{B}{M} + C.N + D.T \quad (1.1)$$

$$\ln\mu = A + B.\ln M + C.N + \frac{D}{T} \quad (1.2)$$

Where A, B, C, D are constants and M is the FAME's molecular weight in g/mol, N is the Number of double bonds available in the fatty acid compound. T is the temperature in Kelvin. Meanwhile ρ is the density and μ is the dynamic viscosity.

Luis Felipe (2012) used different FAMES parameters and formulated other mathematical correlations to calculate density and kinematic viscosity. This can be further illustrated below;

$$\rho = \sum_{i=1}^n w_i (A + \frac{B}{M_i} + C.N_i + D.T) \quad (1.3)$$

$$\ln\mu = \sum_{i=1}^n w_i (A + \ln M_i + C.N_i + \frac{D}{T}) \quad (1.31)$$

Equation 1.4 below is a model derived from the Vogel equation. It was used to compute the kinematic viscosity of saturated FAMES from C6:0 to C24:0, over a wide temperature range (Juan et al., 2013)

$$\ln v_{sat} = a.NC^b + \frac{c.NC^d}{e.\ln NC + f + T} \quad (1.4)$$

Where 'a to f' are parameters of the model and NC being the number of carbon atoms in the hydrocarbon chain.

They went further to use the four parameter equation below, to determine the kinematic viscosity of FAME biodiesel.

$$\ln v = A + B.NC + \frac{C}{T} + \frac{D.NC}{T} \quad (1.5)$$

A, B, C, D are constants used for the calculation. Because of the significance of an accurate and reliable model, this work seeks to develop improved empirical models to

predict the kinematic viscosity of fatty acids biodiesel, as a function of temperature. As a means to overcome this great challenge, three interpolative models are engaged. ANFIS (the Adaptive Neural Inference System), the Response Surface Methodology, and a Mathematical Model are applied. Results from these three models are compared, to select the best model that can be used to gather viscosity data for future applications in engines. Such a method shall be determined from the rate of deviation it produces.

1.3 Research Aims

The main aim of this research is to predict the kinematic viscosity of fatty acid methyl biodiesel, using the following models;

1. ANFIS (Adaptive Neuro fuzzy Inference System),
2. RSM (Response Surface Methodology) and
3. A Mathematical Model.

In broader sense, the study seeks to apply mathematical models to calculate the kinematic viscosity of FAME biodiesel and compare the experimental values of kinematic viscosity, with the predicted values from the above models.

1.4 Thesis Outline

Chapter one gives a synopsis of preceding work done by researchers on this topic and a succinct introduction of biodiesel as a renewable source of energy. Chapter two elaborates some niceties about biodiesel, the advantages and disadvantages of biodiesel and a critical analysis of kinematic viscosity as a property of biodiesel. Chapter three describes the theories of the various models used to predict kinematic viscosity. The methodology applied is examined in chapter 4. Meanwhile chapter five presents the results and discussion on the results, with an outline of the deviations that sandwiched the experimental and predicted results as publicized by the various models. Chapter six gives the conclusion of the entire work in this thesis and some suggestions for future work to be done in this vicinity of research.

CHAPTER 2

BIODIESEL

2.1 Definition

Biodiesel can be referred to a sparkling burning alternative fuel, manufactured from a multiplicity of renewable oil-bearing sources such as vegetable oils and animal fats. Numerous properties of biodiesel are likening to those of petroleum diesel, however biodiesel has copious advantages. Precisely, biodiesel is branded as mono-alkyl esters of long chain fatty acids originating from vegetable oils or animal fats conforming to ASTM D6751 specifications (EN 14214 in Europe) to apply in diesel engines. Biodiesel is applied in several forms, that is, can be blended with petroleum diesel or used directly in its unadulterated form (B100) (Amin et al., 2016).

2.2 Some Major Advantages of Biodiesel

- Types of materials for its production: Because the materials used for its production are renewable, that is animal and vegetable fats, the fuel can be produced over and over, unlike diesel produced from petroleum products, with depleting fossil fuel depots. Petroleum diesel produces more pollution than biodiesel.
- Applicable in all types of car engines: Biodiesel has a unique advantage that older engines using petroleum diesel can switch to biodiesel, with little or no modifications. It is on the basis of this application that biodiesel is persistently replacing fossil fuels as a major source of transport energy.

Some engines utilize pure biodiesel; that is 100% biodiesel (B100). Other engines employ biodiesel blend. For example, B20 is known as 20% blend of biodiesel, containing 80% of diesel made from fossil fuels. Such blend of biodiesel greatly influences the lubrication of engines, leading to long life span of engines and extremely high performance.

- A reduced quantity of Greenhouse Gas is emitted: The quantity of greenhouse gas produced depends on the blend. For instance, B20 reduces CO₂ emission by 15%. Unlike fossil fuels that release toxic gases like carbon dioxide and other into the atmosphere that can cause pollution as well as global warming due to increase in temperature. The advent of biodiesel is basically to shield the environment from excessive heating. Most experts are of the opinion that using biodiesel instead of petroleum diesel reduces greenhouse gases up to about 78%.
- Availability of local materials for production: The fats and oil for biodiesel production are readily obtainable, unlike petroleum diesel that requires the importation of some materials from foreign countries. Today's world has an excessive demand for oil, coal, and gas which cannot be entirely supplied by fossil fuels left on its own. Biodiesel serves as another source of fuel. It is manufactured domestically, hindering the great demand for foreign oil and petrol. Local refineries are used to producing biodiesel. This reduces the desire to import expensive finished products from other countries. The materials used here are equally recycled and renewable.
- Refineries for Biodiesel production are neat: The crude form of oil extracted from the ground is refined before it is used in engines. As the crude oil is refined, toxic chemical like benzene and butadiene are released to the environment, which are harmful to man, plant and animal. Biodiesel being an environmentally fuel, releases less toxic chemicals, with little or no effects, even when the chemicals are spilled onto the ground.
- Eco-friendly and Non-Toxic: During burning, biodiesel produces fewer pollutants and appreciably less carbon output and soot, as compared to petroleum diesel. Biodiesel has a flash point of about 150⁰C whereas that of petroleum diesel is about 52⁰C. This makes biodiesel less flammable. As a matter of fact, biodiesel is easier to store, handle and transported.

- Biodiesel is an Economical fuel: A 30% fuel economy is achieved by vehicles using biodiesel, unlike petroleum diesel engines that make several trips to the fuel stations.
- High Economic Impact: Bio-fuels production plants the world over have employed thousands of people. As the demand for biodiesel increases, more farmers get involved to cultivate the crops used for biodiesel products. Because biodiesel produces less toxic emissions, demand for health care product is less and this influences low cost.
- Non dependence on foreign countries for fossil fuel materials: The non-importation of such materials and use of local materials for biodiesel fuel has caused many nations to save billions of money. This has gone a long way to reduce fuel cost in such nations.
- Health Hazards free environment: Polluted air causes diseases and deaths than any form of pollution. The air emitted by gasoline engines forms smoke that makes several hundreds of people sick. This is greatly done by petroleum diesel. Biodiesel fuel causes less toxic air.

2.3 Disadvantages of Biodiesel

Generally biodiesel fuels have higher values of viscosity, compared to fossil fuel diesel (Nogueira et al., 2010).

- The Quality of Biodiesel differs from one producer to the other: Biodiesel is most often produced from a variety of bio-fuels. Because all bio-fuel crops are not the same, especially with the amount and content of fats in them.
- Unsuitable at lower temperature: At extremely low temperatures, Biodiesel thickens. This causes an increasing its kinematic viscosity and reduces its effectiveness in the engine. As a solution to this thickening problem, biodiesel is

blended with winterized diesel fuel. This goes along way with its higher cloud point at (262K-289K)

- Food Shortage: Consumable vegetable items and crops are used to produce biodiesel, thereby causing food shortages. More demand for biodiesel might sky rocket fats, oil and vegetables prices and create food crisis.
- Increased use of Fertilizers: High yields from crop cultivation is expected as the demand for biodiesel is increasing, therefore fertilizers are used which have devastating effects on the environment. Excessive utilization of fertilizers leads to erosion and land pollution.
- Engine blockage: As a unique advantage of biodiesel, dirt is cleaned from the engine, however this same dirt is collected in fuel filters, which blocks the filters and clogs them.

2.4. The Concept of Viscosity

All liquids possess the characteristic property of viscosity. Viscosity acts as an internal resistance to a fluid in motion. In broader sense, the resistance a fluid generates from being deformed by shear stress or tensile stress is known as viscosity. Patterning to fluids, viscosity is regarded to as “thickness” or “internal friction”. Therefore thin fluids like water have lower viscosity, whereas thicker fluids like biodiesel, shampoo or syrup have higher viscosity. Except super fluids, real fluids are considered viscous, given their resistance to stress. Some fluids have no resistance to shear stress. Such fluids are known as in viscid fluids or ideal fluids. In a nutshell, viscosity is a force that opposes the motion of fluids. Less viscous fluids have relatively greater ease of movement (Tushar et al., 2007).

An amalgamation of three basic factors governs the viscosity of a fluid.

- Intermolecular forces; stronger bonds between fluids molecules make the fluid more viscous.

- Size of the molecules; larger molecules cannot flow past one another like smaller molecules.
- Shape of molecules; molecular shape shows a lot of controversy about viscosity.

This controversy arises because in some situations, linear molecules flow past each other than branched molecules. Meanwhile in some other situations, linear molecules stack on top of one another, than branched molecules.

The design of diesel engines is such that fuel is delivered to the cylinders through the fuel system. The fuel system constitutes components such as; fuel tank, fuel lines fuel pump, fuel filter and fuel injection. When fuel such as biodiesel is pumped into a vehicle, it goes directly into the fuel tank.

When the vehicle is driven, the fuel is pumped out of the fuel tank via the fuel lines and filter to the fuel injector. The injector smartly injects a fine spray of fuel into the cylinders, at exactly the right moment. The cylinder is the combustion chamber. It is the point where compression converts fuel into heat, light and gas. At this point, the fuel is seen to explode. The explosion of fuel in the cylinder pushes the piston outward, producing mechanical motion, which appears linear.

With the aid of a crankshaft, the linear motion of the piston is converted into rotational motion, which turns the wheel of the vehicle. Fuel system components are designed to distribute a certain amount of fuel at a particular rate. This rate of fuel distribution is greatly influenced by viscosity.

Considering that the viscosity of biodiesel fluctuates with temperature changes, it is imperative to note the fuel's viscosity at different temperature points. Numerous reasons account for this;

- It is needed for the convective heat transfer parameter in the fuel system.
- The viscosity values are also needed for thermodynamic analysis in the fuel system.
- The values are equally needed for the fluid mechanics and rheological analysis of the fuel in the system. This is generally regarded as 'Continuum Mechanics.'

Globally accurate viscosity values play an important role in engineering. Viscosity values enable engineers to determine imperative dimensionless groups such as Reynolds number, Prandtl number etc. The power necessary for engine units such as; pump characteristics, storage, atomization or fuel droplet, injection, transportation, fuel passages, and mixing are calculated with appropriate viscosity values.

2.6. Dynamic Viscosity

Shear viscosity or dynamic viscosity of a fluid refers to the resistance of that fluid to shearing flows. In such a fluid flow, adjacent layers of fluids move with different speeds. Consider fluid confined amid two horizontal plates, one immovable and the other moving horizontally with unceasing speed u , as shown.

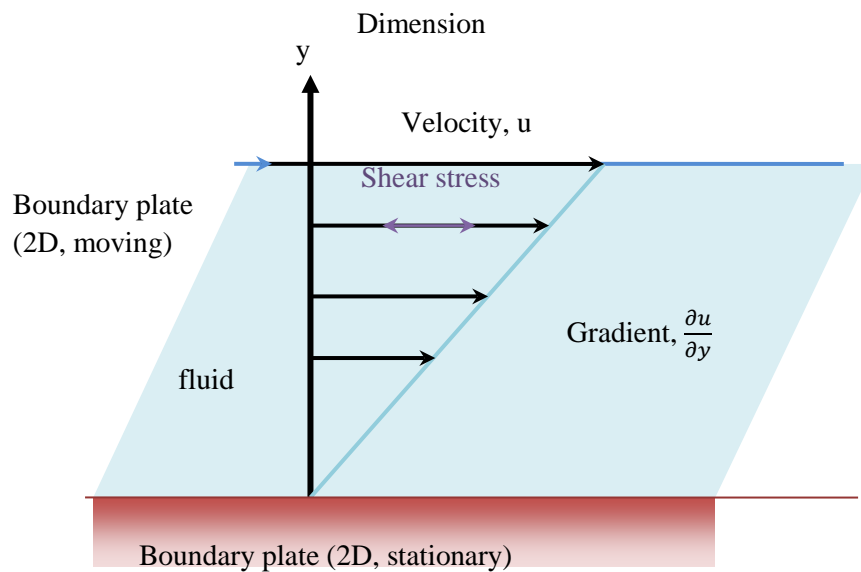


Figure 2.1: Fluid flow between two parallel plates

If the speed of the top plate is small, the fluid particles move parallel to it. The speed of such particles varies linearly from zero at the bottom to u at the top. The fluid between the two plates is made in layers and each layer moves faster than the one beneath it. Frictional forces exist between these layers, creating a force that resists their relative motion. When the top plate starts moving, the fluid generates a force on it. This is reversed, to the motion of the fluid and at the same time creates an equal but opposite force on the down plate.

To keep the top plate moving at a constant speed, an external force is required. Such an external force of size F , is proportional to the speed u and area A of each plate, but inversely proportional to the separation y of the two plates. That is;

$$F = \mu A \frac{\partial u}{\partial y} \quad (2.1)$$

Where μ is a proportionality factor and is known as the dynamic viscosity.

The ratio $\frac{\partial u}{\partial y}$ is the rate of shear deformation or shear velocity. It is the derivative of the fluid speed, in a direction perpendicular to the plates. According to Sir Isaac Newton, the viscous force can be expressed by differential equations, as seen in the illustration below.

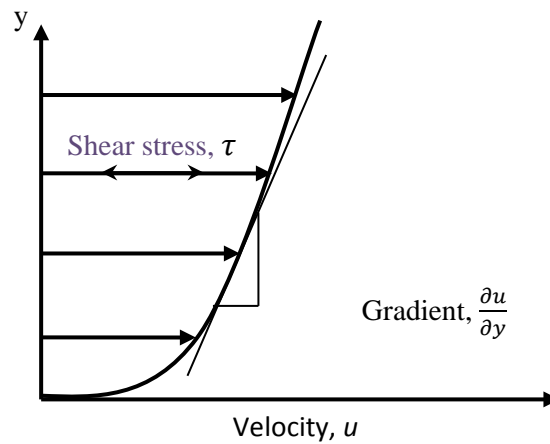


Figure 2.2: Illustration of viscous force differential expression

$$\tau = \mu \cdot \frac{\partial u}{\partial y} \quad (2.2)$$

Where $\tau = \frac{F}{A}$, $\frac{\partial u}{\partial y}$ is the local shear velocity.

The above formula is derived on the basis of a fluid flowing along parallel lines and the y-axis perpendicular to the fluid.

The centipoises (CP) are appropriate units to measure dynamic. It is 1/1000 of poise. Poise is name OF Jean Louis Poiseuille (1799-1869), a French Physicist (Tushar., 2007)

Several other units are used to measure dynamic viscosity;

SI system: $\frac{Ns}{m^2}$, Pa. s or $\frac{kg}{m.s}$, N is the newton and Pa is the Pascal

$$1 \text{ Pa.s} = 1 \frac{Ns}{m^2} = 1 \frac{kg}{m.s}$$

2.7. Kinematic Viscosity

This is one of properties used in the specification of fluids such as fuel and lube oils. It is the ratio of the dynamic viscosity to the density of a substance at the same temperature.

Kinematic viscosity is measured in $\frac{mm^2}{s}$

$$\nu = \frac{\mu}{\rho} \quad (2.3)$$

Where ν is the kinematic viscosity, ρ is the density of the fluid and μ is the dynamic viscosity.

2.8. Factors Affecting Fluid Viscosity

Viscosity is sometimes referred to as flow behavior and is regulated by three basic factors.

- The fuel or substance's inner molecular structure: The closer the molecules are linked together, the more the fuel can resist deformation and consequently the less it will be willing to flow and an effect on viscosity.

- Some liquids like Newtonian liquids do not depend on external forces. When an external force like gravity acts on a fluid, it wipes, pushes or tears the fluid, causing it to flow. Most often, these forces are referred to as shear stress (Thomas et al., 2011).
- Ambient conditions: These conditions emanate when external forces stress a fluid. This results to both temperature and pressure changes. Temperature and pressure changes can cause a fluid to develop different type of flows and consequently viscosity changes. The flow conditions might be laminar or turbulent. Laminar flow is the only flow that can be used to test a fluid's viscosity. In a lamina fluid flow, the fluid moves in very tinny layers, this causes the molecules to be fixed in the layers. . Such a fluid-flow presents an orderly structure.

Such is an enabling condition to measure the viscosity of the fluid.

Though temperature and pressure influence the viscosity of a fluid, temperature has a dominating influence. Viscosity reduces with increase in temperature and increases with decrease in temperature for liquids, unlike gases. Therefore for all liquids, temperature maintains an inverse relationship with viscosity.

When pressure increases, fluid viscosity also increases. However viscosity increases for a pressure change from 0.1 to 30 mPa will produce the same viscosity change as 1K (1⁰C.) For an enormous pressure difference of 0.1 to 200 mPa, a viscosity change of a factor of 3 to 7 occurs. This is experienced for low molecular liquids. For higher viscosity changes, the factor can rise to 2000. Since pressure is inversely proportional to volume

As the pressure increases, the volume pressure in the material structure decreases due to compression. The molecules in the substance come closer and move less freely. The internal frictional force increases, resistance increases and consequently viscosity increases.

CHAPTER 3

THEORIES

3.1 Fuzzy Logic Based Algorithms

Fuzzy logic system (FLS) is a modus operandi of rule-based outcome that utilizes expert System and process control. The structural design of Fuzzy Logic is such that many values logic are created with the true values of variables being real numbers in the range 0 and 1. The one and zero values characterize membership of a member to the set. The design is such that absolute membership is represented by one. Zero doesn't signify any membership.

A measure principle of Fuzzy logic is that it recognizes partial membership. This is usually a number within the range zero and one. The basic concept of Fuzzy theory explains the unique fact that an element shares some degree of membership to a fuzzy set.

FLS has made several successes to practicing engineers especially in the field of modeling and control. Though several difficulties are associated to these successes, FIS has brought a lot of achievements to the engineering field.

FIS comprises three foremost fragments. These include; Fuzzy rules, Membership function of fuzzy rule, and Mechanism of Fuzzy interface.

3.1.1 Analysis with Fuzzy Inference System

Fuzzy system can be analyzed in the following process (Nelles, 2009)

- Fuzzification: Fuzzy logic applies input variables instead of real numbers. Converting a real number into a fuzzy number is fuzzification.
- Knowledge Base: This is made up of a rule and data bases. The fuzzification module functions based on information from the data base. Similarly the rule base feeds information to the defuzzification module. Such information comprises: Fuzzy sets (membership functions). Physical domains and their normalized complements composed the standardization denormalization (scaling) factors.

The control policy appearing as a set of IF-THEN rules is a basic function of the mle

- **Inference Mechanism:** Here the ample value of the control input based on individual contributions of each rule in the rule base is available.
- **Defuzzification:** The contrary of fuzzification is known as defuzzification.

3.2 Types of Fuzzy System

Fuzzy set theory determines FIS. Fuzzy systems are of two kinds:

- **Mamdani fuzzy system:** This is performed in four major stages: Fuzzification of the input variables, rule evaluation, output of the rule outputs, and defuzzification (Castelo and Melin, 2008).
- **Singleton Fuzzy system:** It is a system with a membership function that is one at particular point in the universe and zero everywhere else Sugeno-style fuzzy inference has a lot in common with the Mamdani method. Sugeno alters just one rule consequent (Zah and Howlett, 2006).

3.2.1 Adaptive Network Based Fuzzy Inference System

Adaptive network based fuzzy inference system (ANFIS) is neuron fuzzy technique (Jang, 1993). ANFIS is customarily applied as a principal tool in this work. It is an amalgamation amid neural network and fuzzy logic system. ANFIS's parameters are assessed using two models (Tsukamoto et al., 1979). This shall be obtainable in the architecture of ANFIS. Though ANFIS has some trivial constraints, the ANFIS model bears a resemblance to the Radial basis functions network (RBFN) functionally (Jang and Sun, 1993). ANFIS's methodology is made up of techniques: Hybrid system of fuzzy logic and neural network system.

The adaptive network applications are immediate and immense in various areas. Kinematic viscosity, a principal thermo-physical property of biodiesel is predicted using ANFIS.

3.3 Adaptive Neuro-Fuzzy Inference System (ANFIS)

Fuzzy modeling, Takagi and Sugeno (1985) were able to discover several applications in prediction. ANFIS is a contemporary inference system where a universal approximation is familiarized to signify highly non-linear functions. The adaptive neural network is a network structure comprising numerous nodes, allied via directional links. Each node is categorized by an anode function, with immovable adjustable parameters. During the learning or training face of the neural network, parameter values are determined, which can satisfactorily fit the training data. To a greater extend, ANFIS is a fuzzy Sugeno models positioned in the framework of adaptive systems, in order enthrall learning and adaption (Segeno and Kang, 1988). Considering a first-order Takagi, Fuzzy inference system, a fuzzy model encloses dual rules (Jang and Sun, 1995)

$$\text{Rule 1: If } v \text{ is } V_1 \text{ and } d \text{ is } D_1 \text{ then } f_1 = p_1v + q_1d + r_1 \quad (3.1)$$

$$\text{Rule 2: If } v \text{ is } V_2 \text{ and } d \text{ is } D_2 \text{ then } f_2 = p_2v + q_2d + r_2 \quad (3.2)$$

Where p_1, p_2, q_1, q_2, r_1 and r_2 are linear parameters and V_1, V_2, D_1 , and D_2 are non-linear parameters.

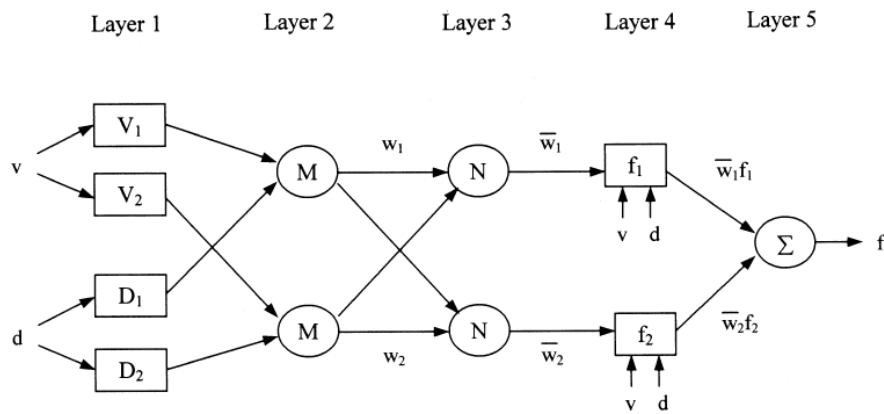


Figure 3.1: Basic ANFIS architecture

Fixed nodes are exemplified here by circles, while squares signify an adaptive node, that is, parameters are altered during adaption or training and O_{ji} donates the output of the i^{th} node in layer j . The whole system architecture entails five layers, viz.; the fuzzy layer, product layer, normalized layer, de-fuzzy layer and total output layer, as shown in Figure 2.1 above.

Layer 1

Each node ‘ i ’ in this layer generates membership grades of a linguistic label. It is the fuzzy layer, in which v and d , are the input nodes. V_1 , V_2 , D_1 and D_2 are the linguistic labels. Expressions are used to shown membership relationship, as stated in the equations below;

$$O_{1,i} = \mu_{v_i}(v); \quad i = 1, 2 \quad (3.3)$$

$$O_{1,j} = \mu_{D,j}(d); \quad j = 1, 2 \quad (3.4)$$

Where $O_{1,i}$ and $O_{1,j}$ denote the output functions and μ_{v_i} and $\mu_{D,j}$ denote the membership functions.

Example 1: The trilateral membership function is engaged by; $\mu_{v_1}(v)$, that is;

$$\mu_{v_i}(v) = \text{Max} \left[\min \left(\frac{v-a_i}{b_i-a_i}, \frac{c_i-v}{c_i-b_i} \right), 0 \right] \quad (3.5)$$

Where, a_i , b_i , and c_i are the parameters of the membership function(MF), prevailing the trilateral membership functions accordingly.

Example 2: If the generalized bell-shaped membership is engaged, $\mu_{v_i}(v)$ is given by

$$\mu_{v_i}(v) = \frac{1}{1 + \left\{ \left(\frac{v-c_i}{a_i} \right)^2 \right\}^{b_i}} \quad (3.6)$$

Where a_i , b_i , and c_i are the parameters of MF, governing the bell-shaped functions accordingly. Parameters in this layer are mentioned as the ‘premise parameters’.

Layer 2

Each node in this layer calculates the ‘firing strength’ of each rule via multiplication

$$O_{2,i} = w_i = \mu_{vi}(v) \mu_{Dj}(d); \quad i=1,2 \quad (3.7)$$

Where $O_{2,i}$ gives the output of layer 2.

Layer 3

The i^{th} node of this layer calculates the ratio of the i^{th} rule’s strength to the sum of all rules’ firing strengths.

$$O_{3,i} = \bar{w} = \frac{w_i}{w_1 + w_2}, \quad i = 1, 2 \quad (3.8)$$

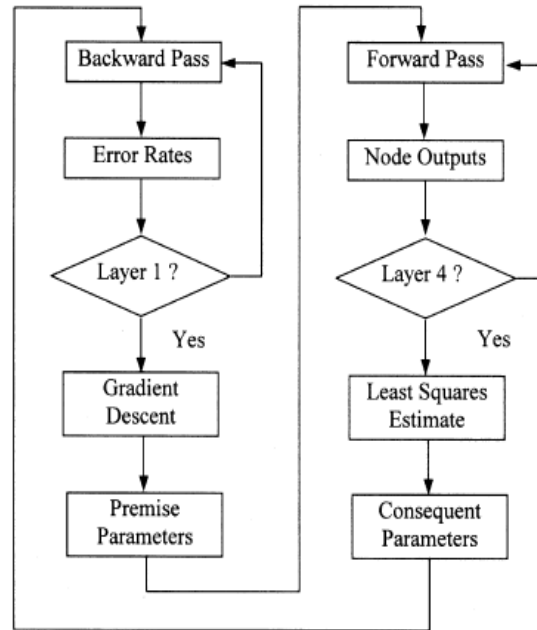


Figure 3.2: A Flowchart of hybrid learning procedure of ANFIS

Where O_{4i} donates the layer 4 output. In this layer, p_i , q_i , and r_i are called linear parameters or consequent parameters.

Layer 5

The single node in this layer is a circle of nodes labelled ' Σ ' that computes the 'overall ouput' as the summation of all incoming signals i.e.

$$O_{5,i} = \sum_i w_i f_i = \frac{\sum_i w_i f_i}{\sum_i w_i} \quad i=1,2 \quad (3.91)$$

The first and fourth layers represent adaptive layers in ANFIS architecture. The adjustable parameters are equally known as principle parameters in the first layer and consequent parameters in the fourth layer. The main duty associated with the learning is to turn all adjustable parameters, to allow the ANFIS output resemble the training data. To improve the rate of convergence, a hybrid learning algorithm (Figure 3.1) combining the least square method and gradient descend method is adopted. The purpose of the least square is to optimize the consequent parameters, with the premise parameters fixed. As soon as the optimal consequent parameters are found, the gradient descend method is used to adjust optimally the premise parameters corresponding to the fuzzy sets in the input domain. The output of ANFIS is calculated by employing consequent parameters. The output error is used to adapt the premise parameters via a standard back propagation algorithm or hybrid optimum.

3.4 Response Surface Methodology

Response surface methodology (RSM) is an assembly of mathematical and statistical modeling technique applied for multiple regression and analysis and to quantify the relationships between one or more measured responses and the vital input measure.

RSM can be described as an emperical modeling system employed for developing ,improving, and optimizing complex process. (Montgomery and Douglas, 2005). RSM has the advantage of reducing the number of experimental runs, which is sufficient to provide statistically acceptable results. Tiwari et al. (2011) used RSM to optimze biological

production process from Jatropha oil. At last, the tool was used to optimize biodiesel production of Sesamum indicum oil.

A general linear interaction model is shown in the equation below, which accounts for the independent parameters with their interaction effects was considered in this study. As shown in the equation below, where x_i s are the levels of the factors under study, Y is the predicted response of the process (% yield of BDF), n is the number of factors, β_0 is the intercept term, β_i , and β_{ij} are the linear and interactive coefficients respectively.

The method of least squares was employed to ascertain the values of the model parameters and analysis of variance (ANOVA) was applied to establish their statistical significance at confidence level of 95%

$$Y = \beta_0 \sum_{i=1}^n \beta_i x_i + \sum_{i=1}^{n-1} \sum_{j=i+1}^n \beta_{ij} x_i x_j \quad (3.92)$$

3.5 Mathematical Correlation

The temperature dependence of viscosity for a good number of methyl fatty acids has been expressed in several models, as seen in the literature review. These expressions include three-parameter derivations of the well-known Andrade equation (Vogel, 1992). The Vogel equation is a three-parameter model given by;

$$\ln \mu = A + \frac{B}{C+T} \quad (3.93)$$

In the above equation, A , B and C are modifiable parameters while T is the temperature in Kelvin. When the viscosity of the methyl fatty acid that is the component of the biodiesel is determined, a mixing rule is required to approximate. A simple mixing rule that assumes ideal mixture is shown in the equation below.

$$\ln \mu_B = \sum_{i=1}^n x_i \ln u_i \quad (3.94)$$

Where; (x_i) is the mass fraction of the i^{th} alkyl ester, n is the number of esters present in the mixture u_i and u_b are the viscosities.

Fatty acid methyl esters are divided into saturated and unsaturated forms. The saturated form has been carefully selected from the range C6:0, C8:0, C10:0, C12:0, C14:0, C16:0, C18:0, C20:0, C22:0, C24. Meanwhile the unsaturated has been chosen from C14.1, C16.1, C18, and C18.2 C18.3. Some values of kinematic viscosity and density at the same temperature have been converted to kinematic viscosity, by using the equation;

$$v = \frac{\mu}{\rho} \quad (3.95)$$

In equation 3.95, v is the kinematic viscosity, μ is the dynamic viscosity and ρ is the density in kg/m^3

With the four numeric constants calculated from previous equations, the equation below can be used to calculate the kinematic viscosity

$$\ln \mu = -2.915 - 0.158z + \frac{492.12}{T} + \frac{108.35Z}{T} \quad (3.96)$$

Where z is the particular FAMES taken into consideration. The following equation is also applied to calculate the kinematic viscosity of FAMES, ranging from C6:0 to C24:0, over a wide range of temperature wherein; v_{sat} is the kinematic viscosity in mm^2/s of the saturated FAMES, NC is the number of carbon in the hydrocarbon chain, T is the temperature in Kelvin and a, b, c, d, f , are the parameters of the model, whose values are given as shown

$$\ln v_{sat} = a.NC^b + \frac{c.NC^d}{e.\ln NC + f + T} \quad (3.97)$$

CHAPTER 4

METHODOLOGY

Several steps were surveyed in this thesis to develop predictive models for the kinematic viscosity of fatty acid methyl esters biodiesel. The main steps that steered to the realization of the predicted results are enumerated;

4.1 The Experimental Database

The databases for this study were formed from results reported in the literature. The following tables illustrate the data used for prediction. 251 experimental points for unsaturated FAMES and 496 experimental data points for saturated FAMES, making a total of 747 were obtained from numerous scientific publications, and used to guesstimate the kinematic viscosity of FAME biodiesel.

Table 4.1: Sources of Data from Literature Reviews

FAMES	MEASURING	REFERENCES
C6:0	Temperature dependent of viscosity of biodiesel	Yuan et al., (2009)
C18:0	fuels	
C10:0	Kinematic viscosity of biodiesel components, fatty	Knothe et al.,(2007)
C12:0	Acid alkyl esters and related compounds at low	
C18:0	Temperature	
C18:1		
C18:3		
C6:0	Viscosities and densities of some methyl esters of some	Liew &Seng, (1992)
C8:0	n- alkanoic acids	
C8:0	-Densities and viscosities of fatty acid methyl and esters	Pratas et al., (2010)
C18:0	-Group contribution model for predicting viscosity of	Ceriani et al., (2007)
C12:0	fatty	
C14:0	Compounds	Yuan et al., (2009)
C14:1	-Density and viscosity of biodiesel as a function of	Ramerirez (1999)
C16:1	temperature	
C18:2		
C16	-Esters of naturally occurring fatty acids, physical	Bonhorst et al.,
C12	properties of	
C10	Fatty acids of methyl, propyl and isopropyl esters.	(1948)
C20	-Evaluation of predictive models for the viscosity of	

Table 4.2: Kinematic Viscosity (mm²/s) of Unsaturated FAMES

T (K)	C14.1	C16.1	C18.1	C18.2	C18.3
263.15	9.92	14.77	21.33	14.1	10.19
268.15	8.37	12.19	17.22	11.8	8.87
273.15	7.01	10.15	14.03	9.84	7.33
278.15	6.13	12.19	11.66	8.47	6.59
				8.322	6.965
				8.46	6.9658
				8.3219	6.966
283.15	5.35	7.33	9.869	7.3	5.53
				7.236	6
				7.2365	6.176
					6.1773
					6.1774
288.15	4.73	5.341	8.51	6.43	5.524
		6.38	8.49	6.355	5.14
				6.43	5.5241
293.15	4.13	4.723	7.33	5.61	4.57
		5.56	7.379	5.622	4.972
			7.23	5.58	4.84
			7.38	5.61	4.9722
				5.6194	
298.15	3.71	4.94	6.44	5.03	4.07
		4.214	6.472	5.017	4.501
			6.47		4.5011
303.15	3.37	3.806	5.72		

Table 4.2: Continued

				4.5079	4.0989
					4.0973
308.15	3.04	3.96	5.08	4.08	3.32
		3.432	5.099	4.075	3.75
					4.0504
					3.7504
313.15	2.73	3.064	4.51	3.65	3.09
		3.67	4.573	3.703	3.298
			4.45	3.64	3.27
			4.721	3.702	3.14
					3.2898
		2.85	4.125	3.383	3.028
			4.123	3.103	3.0284
				3.102	
				3.3826	
323.15		2.57	3.742	3.103	2.811
333.15		2.229	3.121	2.644	2.434
					2.263
338.15					2.4343
343.15		1.918			2.1
		2.06	2.871	2.453	2.09
		1.918	2.651	2.2832	2.1002
			2.6	2.25	2.0903
			2.457	2.132	1.96
		1.792		2.1507	1.9621
					1.9598

Table 4.3: Kinematic Viscosity (mm²/s) of Saturated FAMEs Data

T (K)	C6:0	C8:0	C10:0	C12:0	C14:0	C16:0	C18:0
263.15			5.5				
			5.4				
			4.04				
268.15			4.68				
273.15	2.31		4.04		7.0		
278.15			3.378	5.45			
			3.49				
			3.378				
283.15	1.179	1.967	3.01	4.654			
		1.913	3.014	4.635			
		1.931	3.014	4.79			
				4.364			
288.15	1.084	1.772	2.689	4.093			
		1.769	2.708	4.094			
			2.71	4.07			
293.15	1.01	1.61	2.421	3.627	5.201		
	1.012	1.59	2.437	3.54			
	1.011	1.628	2.449	3.641			
		1.627	2.49	3.63			
			2.45	3.640			
			2.448				
298.15	0.9412	1.471	2.196	3.225	4.611		
		1.504	2.227	3.261	4.6105		

Table 4.2: Continued

			2.23	3.29	
				3.2614	
303.15	0.8822	1.368	2.004	3.892	4.12
		1.396	2.037	2.942	4.1643
		1.390	2.05	2.95	
			2.036	2.942	
				2.942	
308.15	0.830	1.262	1.832	2.618	3.698
		1.3	1.871	2.668	3.697
		1.3001	1.87	2.69	
			1.871	2.668	
310.95	0.81	1.207	1.765	2.487	3.456
313.15	0.785	1.17	1.686	2.384	3.338
	0.785	1.16	1.69	2.433	3.3
		1.215	1.726	2.431	2.73
		1.19	1.71	2.41	3.3381

Table 4.3 Continued

T (K)	C6	C8	C10	C12	C14	C16	C18	C20	C22
313.15				2.43	3.0303				
				2.433	3.23				
	0.7422	1.099	1.566	2.139	3.0303	2.977	5.241		
		1.138	1.589	2.229		2.9766	5.2451		
		1.138		2.228					
318.15	0.7014	1.028	1.452	2.014	2.764	3.602	4.706	5.736	
		1.069	1.485	2.05	2.763		4.705	5.737	
		1.06	1.184						
328.15	0.6668	0.966	1.353	1.859	2.533	3.28	4.254	5.154	
		1.006	1.384	1.893	2.5327		3.666	5.153	
			1.383				4.2537		
	0.632		1.263	1.724	2.323	2.998	3.861	4.23	5.692
333.15	0.6332		1.276	1.732	2.33	3.001	3.666	4.657	5.691
			1.294	1.724	2.329		3.8611		
			1.291	1.755					

Table 4.4: Names and formulae of the various FAMES

Fatty acid	Methyl ester name	Methyl ester formula	M(g/mol)
C6:0	Methyl hexanoate	$C_7H_{14}O_2$	130.87
C8:0	Methyl caprylate	$C_9H_{18}O_2$	158.2380
C10:0	Methyl caprate	$C_{11}H_{22}O_2$	186.2912
C12:0	Methyl laurate	$C_{13}H_{26}O_2$	214.3443
C14:0	Methyl myristate	$C_{15}H_{30}O_2$	242.3975
C16:0	Methyl palmitate	$C_{17}H_{34}O_2$	270.4507
C18:0	Methyl steareate	$C_{19}H_{38}O_2$	298.5038
C20:0	Methyl arachidate	$C_{21}H_{42}O_2$	326.5570
C22:0	Methyl behenate	$C_{23}H_{46}O_2$	354.6101
C24:0	Methyl lignocerate	$C_{25}H_{50}O_2$	382.663
C14:1	Methyl myristoleate	$C_{15}H_{28}O_2$	240.387
C16:1	Methyl palmitoleate	$C_{17}H_{32}O_2$	268.4348
C18:1	Methyl oleate	$C_{19}H_{36}O_2$	293.4879
C18:2	Methyl linoleate	$C_{19}H_{34}O_2$	294.4721
C18:3	Methyl linolenate	$C_{19}H_{32}O_2$	292.4562

4.2 Empirical models

The kinematic viscosity of fatty acid methyl esters was modeled using three empirical models.

- i) Adaptive Neural Fuzzy Inference System (ANFIS)
- ii) Response Surface methodology
- iii) Mathematical correlation.

Three input parameters, the number of carbon (NC) atoms, number of hydrogen (NH) atoms and temperature in Kelvin FAMES were used to get one output, viscosity. The available data was normalized, for accurate results.

Table 4.5: Limits for the input and output parameters for the models.

Input value	Limit Value	unit
Temperature	263.15-372.15	[K]
Number of hydrogen	14-44	
Number of carbon	7-23	-
Output value		
Kinematic viscosity	0.457-14.77	

CHAPTER 5

RESULTS AND DISCUSSIONS

5.1 Method of Applications of ANFIS for the Prediction of Kinematic Viscosity of Saturated Fatty Acid Methyl Biodiesel

The anticipated ANFIS methodology to predict the kinematic viscosity of fatty acid methyl biodiesel at different temperatures, using the input parameters of number of carbon atoms, number of hydrogen atoms and temperature is shown in the figure below. The model was trained with part of the database derived from the literature review. A total of 496 data point for saturated fatty methyl acid was used. The database was split into training data, 60%, testing data, 20%, and checking data, 20%.

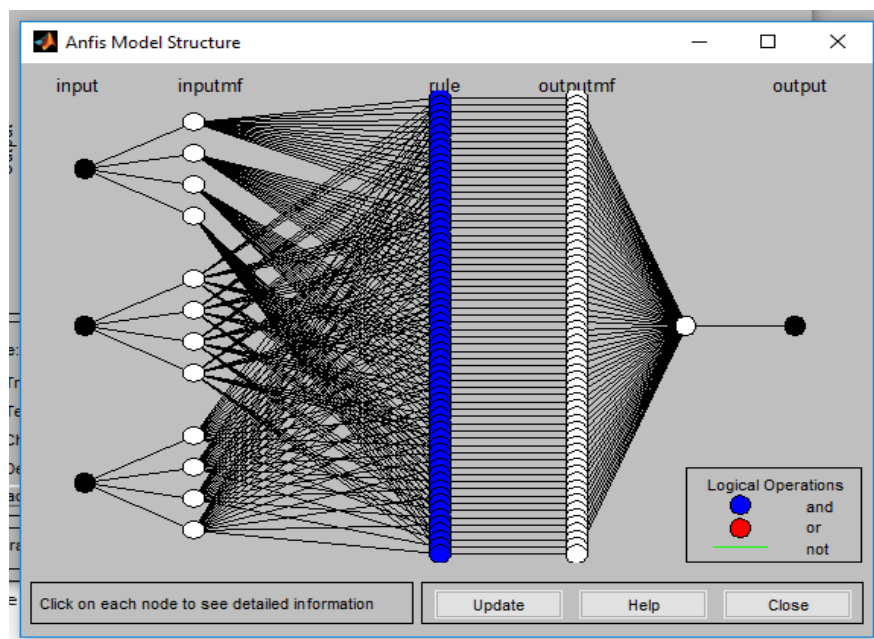


Figure 5.1: ANFIS architecture for kinematic viscosity of FAMES biodiesel

In this work, the best number of membership function for each output was determined at 5. The membership grades take the Gaussian-shaped membership functions and the output part of each rule uses a linear defuzzifier formula, which was found by trial and error methods. This is shown in tables 5.1 and 5.2. The generation ANFIS is tested by two methods, the hybrid and back-propagation. The results are shown in table 5.1 and 5.2. The results show that the training error in the hybrid method is lower than the training error in the back- propagation method. Therefore the hybrid method is used in this study. The able below shows the system parameters of ANFIS model for kinematic viscosity of FAMES biodiesel.

Table 5.1: The ANFIS information by the hybrid optimum method

Mf No	Mf Types	Mf Output	Method	Training Error	Testing Error	Checking Error
2	Trimf	Constant	Hybrid	0.33291	0.43983	0.43481
3	Trimf	Constant	Hybrid	0.16671	0.28781	0.26579
4	Trimf	Constant	Hybrid	0.14029	0.33428	0.16594
5	Trimf	Constant	Hybrid	0.11636	0.26725	0.39913
6	Trimf	Constant	Hybrid	0.11911	0.28379	0.48613
7	Trimf	Constant	Hybrid	0.11070	0.33434	0.33529
2	Trimf	Linear	Hybrid	0.15406	0.23444	0.20197
3	Trimf	Linear	Hybrid	0.11071	10.9980	5.9279
4	Trimf	Linear	Hybrid	0.11306	1.3098	0.88065
5	Trimf	Linear	Hybrid	0.09714	0.68897	0.49366
2	Trapmf	Constant	Hybrid	0.59331	0.79756	0.77103
3	Trapmf	Constant	Hybrid	0.53361	0.79087	0.57732
4	Trapmf	Constant	Hybrid	0.4550	0.76515	1.20080

Table 5.1: Continued

2	Trapmf	Linear	Hybrid	0.1483	0.27376	0.7895
3	Trapmf	Linear	Hybrid	0.1472	0.25454	0.25743
4	Trapmf	Linear	Hybrid	0.1264	0.59285	1.0309
5	Trapmf	Linear	Hybrid	0.11704	0.49173	0.20858
6	Trapmf	Linear	Hybrid	0.1039	0.6813	0.33050
7	Trapmf	Linear	Hybrid	0.10874	0.60439	0.19054

Trials were equally made, using back-propagation to get the minimum testing, training and checking errors for the Trimf and Trapmf functions of ANFIS. This is shown in table below.

Table 5.2: The ANFIS information by the back-propagation optimum method

Optimum Method	Number of MF	MF Type	MF Output	Training Error	Testing Error	Checking Error
Back-propagation	2	Trimf	Constant	1.7014	2.029	1.9136
Back-propagation	3	Trimf	Constant	1.7639	2.1074	2.2625
Back-propagation	4	Trimf	Constant	2.0135	2.3883	2.3596
Back-propagation	5	Trimf	Constant	2.0729	2.4725	2.4211
Back-propagation	2	Trimf	Linear	0.8811	0.96981	0.86706
Back-propagation	3	Trimf	Linear	0.71673	0.75455	0.65542
Back-propagation	4	Trimf	Linear	0.55896	0.5866	0.57048
Back-propagation	5	Trimf	Linear	0.55263	0.54649	0.56909

Table 5.3: System parameters of the ANFIS model

ANFIS model parameter	
Number of nodes	158
Number of linear parameters	256
Number of non-linear parameters	36
Total number of parameters	292
Number of training data pairs	276
Number pairs of checking data	36
Number of fuzzy rules	64

Table 5.4 Summarizes the ANFIS information and error values which are used in this study to predict the kinematic viscosity of saturated fatty acid methyl biodiesel. The function used here is Trimf. The ANFIS network was able to achieve training and checking of the lowest RMSE (root mean standard error), for kinematic viscosity of FAME biodiesel.

Table 5.4: predicting error for saturated FAMEs

Epoch	300
Training Error	0.9714
Checking Error	0.49366
Testing Error	0.68897

The figure below shows the rule viewers of the kinematic viscosity, indicating the value of the various inputs of the ANFIS models and possible output. The kinematic viscosity is predicted by varying the input parameters, amongst the number of carbon atom, number of hydrogen atoms, and the temperature, to the developed ANFIS model.

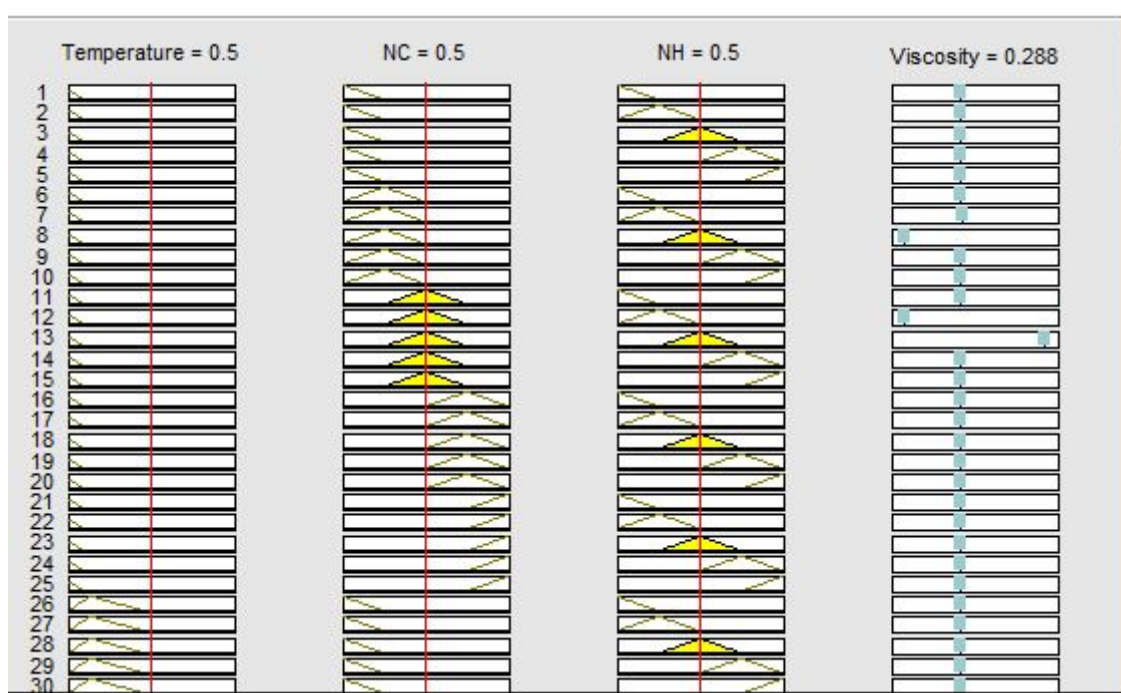


Figure 5.2: Rule viewer of ANFIS model for Saturated FAME biodiesel

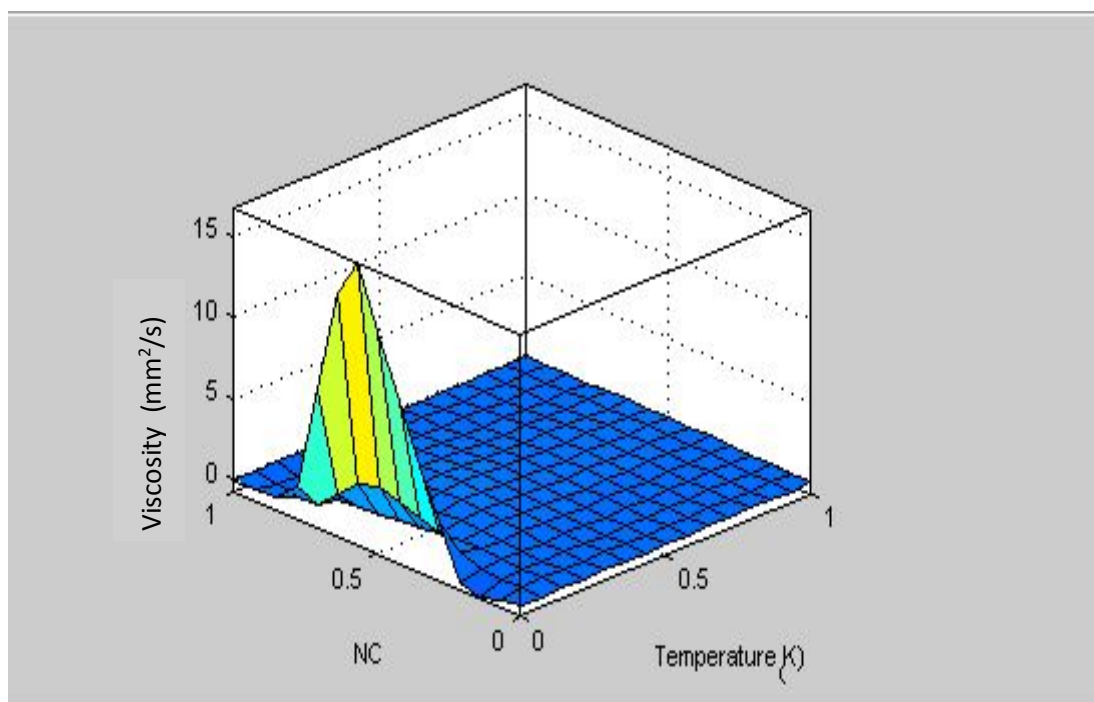


Figure 5.3: Surface viewer of ANFIS model for saturated FAME biodiesel

The three D surface plots of the kinematic viscosity, temperature and number of carbon atoms of FAME biodiesel is shown in Figure 5.3 beneath. Standard units of Kelvin (K) and mm^2/s have been used to measure temperature and viscosity respectively.

5.2. Modeling the kinematic viscosity of saturated fatty acid methyl biodiesel

The figure underneath shows the results of fitting the predicting and experimental results or the kinematic viscosity of fatty acid methyl biodiesel, using linear regression. The graph shows that there is proper fitting of the predicted values by the adopted methodology.

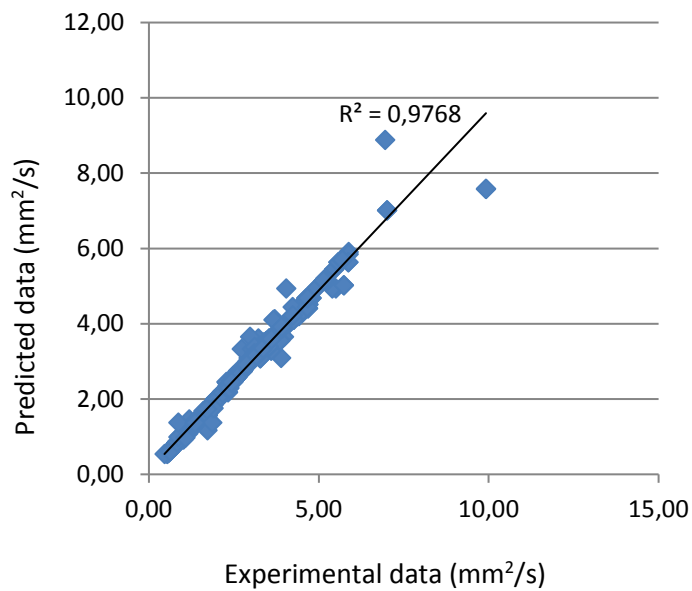


Figure 5.4: Plot of experimental data versus ANFIS predicted data for saturated FAME

Table 5.5: Comparing experimental and ANFIS results for saturated FAME

T (K)	NC	NH	Kinematic Viscosity (mm ² /s)		Absolute
			EXP	ANFIS	Error
					(%)
353.15	11	22	1.014	1.02	0.59
343.15	9	18	0.8525	0.84	1.47
313.15	9	18	1.2	1.2	0
298.15	11	22	2.23	2.18	2.24
313.15	7	14	0.7852	0.78	0.66
293.15	11	22	2.437	2.45	0.53
313.15	17	34	4.32	4.2	2.78
313.15	15	30	3.23	3.33	3.1
313.15	9	18	1.215	1.2	1.23
358.15	11	22	0.91107	1.02	1.2
372.05	17	34	1.905	1.75	8.14
348.15	9	18	0.7718	0.79	2.36
293.15	11	22	2.49	2.45	1.61
353.15	11	22	0.9927	1.02	2.75
318.15	17	34	3.9766	3.65	8.21
313.15	19	38	5.61	5.63	0.36
363.15	21	42	2.793	2.78	0.47
348.15	9	18	0.8161	0.79	3.2
373.15	23	46	2.8714	2.91	1.34
293.15	13	26	3.54	3.61	1.2
348.15	17	34	2.355	2.54	7.86
293.15	11	22	2.421	2.45	1.2
263.15	15	30	9.92	7.58	2.77
313.15	17	34	4.4136	4.2	4.84
298.15	11	22	2.196	2.61	18.85

Table 5.1: Continued

T (K)	NC	NH	Kinematic Viscosity (mm²/s)		Absolute Error (%)
			EXP	ANFIS	
343.15	19	38	2.323	2.35	0.81
338.15	11	22	3.2271	3.2	0.84
353.15	15	30	1.213	1.21	0.3
313.15	17	34	1.732	1.68	3
288.15	13	26	4.38	4.2	2.74
328.15	9	18	4.094	4.07	0.59
313.15	13	26	0.9663	0.99	2.5
310.3	13	26	2.431	2.45	0.78
310.95	15	30	2.487	2.61	4.5
333.15	23	46	3.456	3.49	0.98
308.15	13	26	5.6912	5.69	0.02
310.95	17	34	2.69	2.74	1.86
333.15	13	26	4.688	4.51	3.8
313.15	13	26	1.732	1.73	0.12
283.15	13	26	2.4331	2.45	0.69
318.15	15	30	4.79	4.68	2.3
363.15	21	42	3.03	3.01	0.66
313.15	15	30	2.7926	2.78	0.45
283.15	13	26	3.23	3.33	3.1
348.15	19	38	4.79	4.68	2.3
343.15	21	42	3.86	3.87	0.26
348.15	21	42	3.93	3.87	1.53
283.15	11	22	2.45	2.45	0
323.15	9	18	1.72	1.71	0.58

Table 5.1: Continued

T (K)	NC	NH	Kinematic Viscosity (mm²/s)		Absolute Error (%)
			EXP	ANFIS	
308.15	15	30	1.732	1.68	3
323.15	13	26	3.698	3.7	0.05
338.15	11	22	2.05	1.99	2.93
313.15	11	22	1.2131	1.21	0.26
343.15	13	26	1.72	1.71	0.58
328.15	19	38	1.51	1.53	1.32
333.15	13	26	4.2537	4.1	3.61
363.15	19	38	1.756	1.73	1.48
343.15	23	46	2.367	2.29	3.25
348.15	9	18	4.672	4.68	0.17
273.15	11	22	0.8103	0.79	2.51
313.15	9	18	4.04	3.94	2.48
343.15	15	30	1.16	1.2	3.45
328.15	17	34	1.95	1.99	2.05
343.15	9	18	3.28	3.08	6.1
283.15	7	14	0.819	0.84	2.56
343.15	15	30	1.179	1.37	16.2
343.15	17	34	1.9955	1.99	0.28
313.15	13	26	2.5	2.54	1.6
338.15	15	30	2.4331	2.45	1.69
353.15	11	22	2.152	2.18	2.8
333.15	13	26	1.0137	1.02	0.62
303.15	15	30	1.724	1.73	0.6
353.15	21	42	4.1643	4.12	1.06

Table 5.1: Continued

T (K)	NC	NH	Kinematic Viscosity (mm ² /s)		Absolute Error (%)
			EXP	ANFIS	
288.15	19	34	6.355	6.28	1.18
318.15	19	34	3.103	3.3	2.35
278.15	15	28	6.13	7.78	26.92
333.15	19	32	2.263	2.49	10.03
298.15	19	36	6.472	6.52	0.74
293.15	19	32	4.84	4.95	2.27
313.15	19	32	3.298	3.27	0.85
353.15	19	34	1.966	2.03	3.26
263.15	15	28	9.92	13.8	3.11
278.15	19	34	8.46	8.46	0
323.15	19	36	3.741	3.69	1.36
343.15	19	34	2.25	2.27	0.89
323.15	19	36	3.742	3.69	1.39
328.15	19	32	2.629	2.6	1.1
308.15	15	28	3.432	3.56	3.73
289.15	19	34	5.017	6.12	21.99
313.15	19	32	3.298	3.27	0.85
293.15	19	34	5.58	5.09	8.78
308.15	15	28	3.96	3.56	10.1
363.15	19	32	1.649	1.51	8.43
348.15	19	32	1.9621	2.06	4.99
343.15	19	32	2.1002	2.22	5.7
333.15	19	32	2.4343	2.64	8.45
293.15	19	34	5.61	5.58	0.53

Table 5.1: Continued

T (K)	NC	NH	Kinematic Viscosity		Absolute
			(mm ² /s)		Error
			EXP	ANFIS	(%)
268.15	19	36	17.22	17	1.28
263.15	19	36	21.33	19.7	7.64
308.15	19	34	4.075	4.05	0.61
303.15	19	34	4.5079	4.53	0.49
313.15	19	32	3.14	3.27	4

5.3 Method of Applications of ANFIS for the Prediction of Kinematic Viscosity of Unsaturated Fatty Acid Methyl Biodiesel

The anticipated ANFIS methodology to predict the kinematic viscosity of unsaturated fatty acid methyl biodiesel at different temperatures, using the input parameters of number of carbon atoms, number of hydrogen atoms and temperature is shown in the figure below. The model was trained with part of the database derived from the literature review. A total of 251 data points for unsaturated fatty methyl acid was used. The database was split into training data, 60%, testing data, 20%, and checking data, 20%.

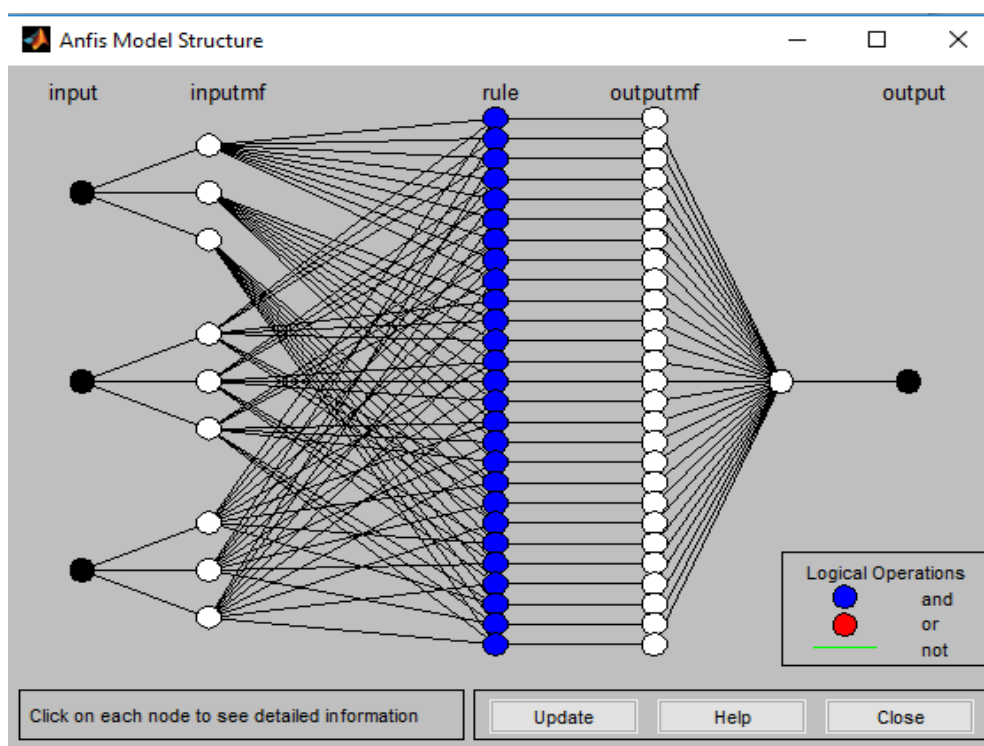


Figure 5.5: ANFIS architecture for predicting the kinematic viscosity of FAMES

For the unsaturated FAMEs, the best number of membership functions for each input was determined at 3, the membership grades take the Gaussians-shaped membership functions and the output part of each rule uses a linear DEFUZZIFIER formula, which is found by trial and error methods (Table 5.6 and table 5.7). To determine the minimum errors, two functions, hybrid and back-propagation were tested for the generation ANFIS.

Table 5.6: The ANFIS information by the hybrid optimum method

Optimum Method	Number Of MF	MF Type	MF Type (output)	Training Error	Testing Error	Checking Error
Hybrid	2	Trimf	Linear	0.62898	0.73687	2.5308
Hybrid	3	Trimf	Linear	0.60421	0.57664	0.78638
Hybrid	4	Trimf	Linear	0.54734	0.64909	0.94632
Hybrid	5	Trimf	Linear	0.56753	0.56872	1.1362
Hybrid	6	Trimf	Linear	0.55784	0.61186	1.1314
Hybrid	2	Trimf	Constant	1.4249	1.5897	2.4055
Hybrid	3	Trimf	Constant	0.94804	1.1305	1.5408
Hybrid	4	Trimf	constant	0.69681	0.77001	1.1707
Hybrid	5	Trimf	Constant	0.63584	0.62365	1.2601
Hybrid	6	Trimf	constant	0.61048	0.5667	1.191
Hybrid	7	Trimf	constant	0.59931	0.54479	1.162
Hybrid	2	Trapmf	Linear	0.79487	0.97836	1.3713
Hybrid	3	Trapmf	Linear	0.65692	0.64865	1.097
Hybrid	4	Trapmf	Linear	0.61419	0.60227	1.2519
Hybrid	2	Gaussmf	Linear	0.6692	0.71048	0.96026
Hybrid	3	Gaussmf	Linear	0.6024	0.56484	1.1797

Table 5.7: ANFIS information by back-propagation optimum method

Optimum Method	Number Of MF	MF Type	MF Type (output)	Training	Testing	Checking
Back-propagation	2	Trimf	Linear	1.8383	1.9646	2.8259
Back-propagation	3	Trimf	Linear	1.3056	1.5673	1.9696
Back-propagation	4	Trimf	Linear	0.84101	0.95932	1.4326
Back-propagation	5	Trimf	Linear	0.89299	0.87957	1.3821
Back-propagation	2	Trimf	Constant	4.8394	4.3361	5.5889
Back-propagation	3	Trimf	Constant	5.2151	4.7405	6.049
Back-propagation	4	Trimf	Constant	5.5809	5.1553	6.5219
Back-propagation	5	Trimf	constant	4.8394	4.3361	5.5889

As seen in the table above, trial errors for hybrid as an optimum method are minimal than those of back-propagation. Consequently, the optimum method hybrid is used to generate the ANFIS, for the prediction of the kinematic viscosity of the unsaturated fatty acid methyl biodiesel.

Table 5.8: System Parameters of the ANFIS Model

ANFIS model parameter	
Number of linear parameter	108
Number of nonlinear parameters	27
Total number of parameters	135
Number of training data pairs	164
Number of testing data pairs	109
Number of checking data pairs	22
Number of fuzzy rules	27

ANFIS information used to predict the kinematic viscosity of FAME, by the hybrid optimum method

Table 5.9: Indicates the ANFIS error that was used to predict the kinematic viscosity of FAMEs biodiesel

Unsaturated Fatty acid methyl biodiesel	
Epoch	300
Training error	0.60421
Testing error	0.57664
Checking error	0.78638

The figure below shows the rule viewer of the kinematic viscosity of unsaturated FAMES. It indicates the various inputs of the ANFIS model. The kinematic viscosity (output), can be predicted by varying the input parameters of number of carbon atoms, number of hydrogen atoms, and temperature, in order to develop the ANFIS model.

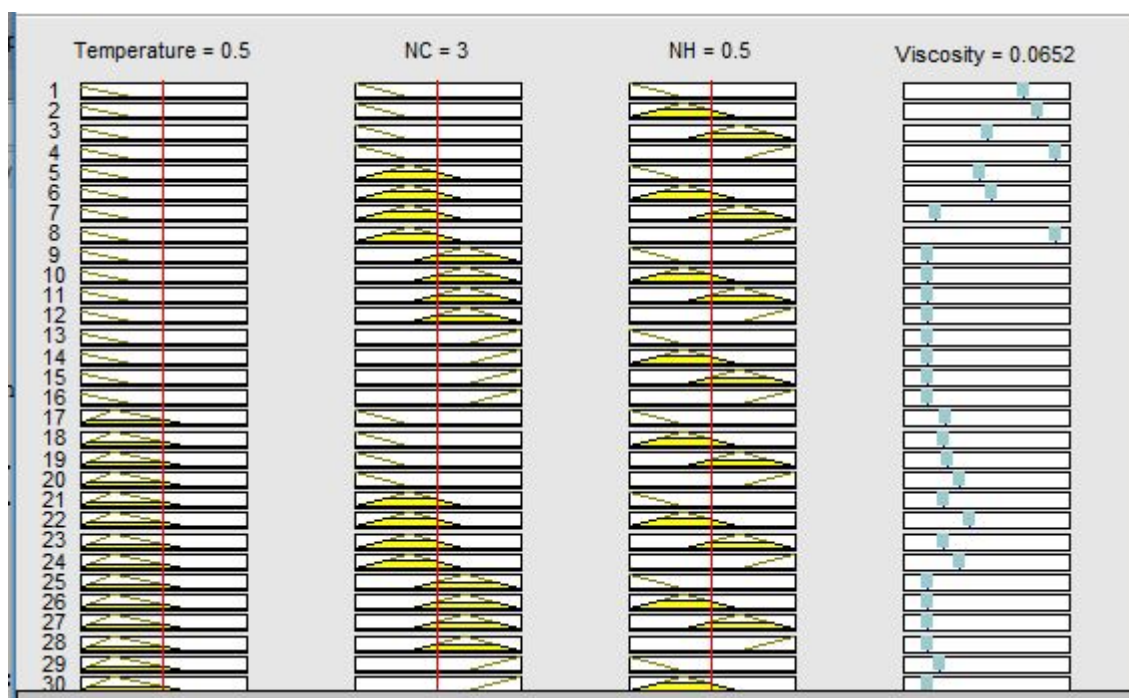


Figure 5.6: Rule viewer of ANFIS model for the kinematic viscosity of unsaturated fatty acid methyl biodiesel

The 3D surface plots of kinematic viscosity of unsaturated fatty acid methyl biodiesel against temperature and number of carbon atoms is displayed in the figure below

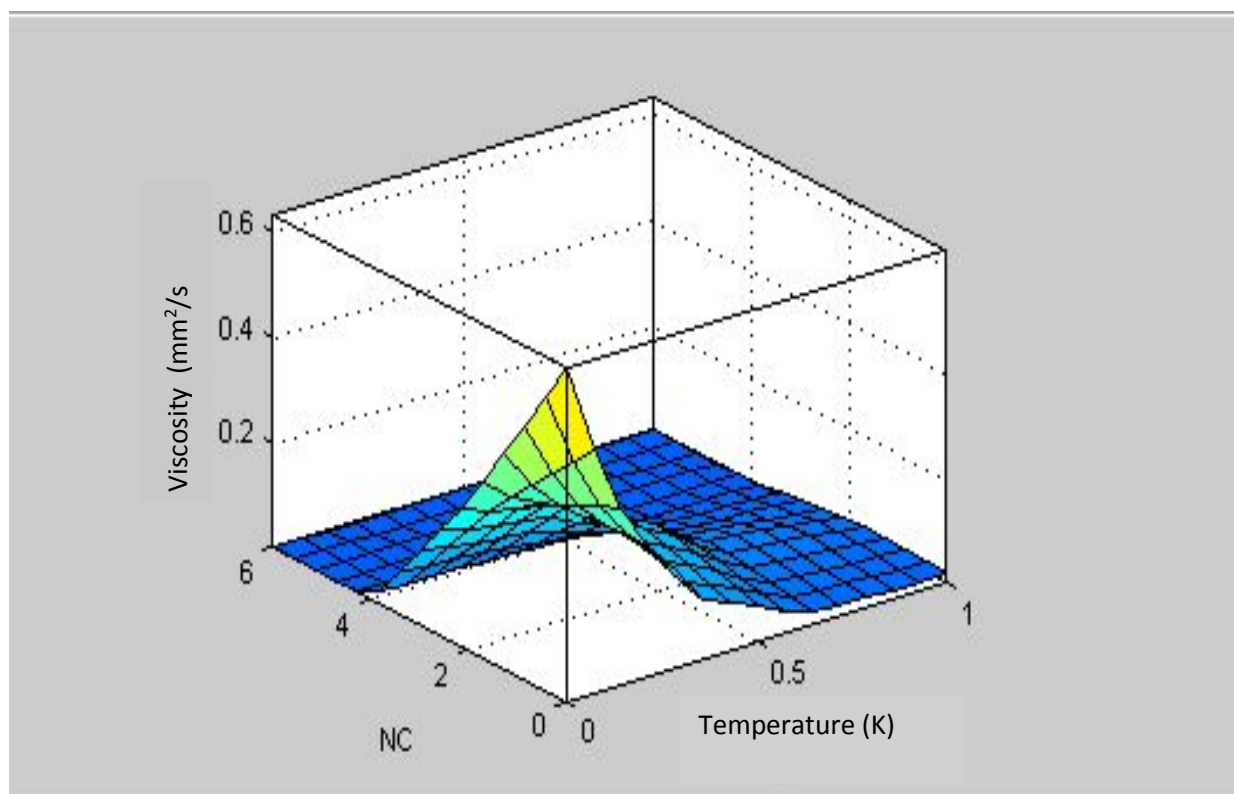


Figure 5.7: Surface viewer of ANFIS model for kinematic viscosity of unsaturated FAMES

5.4 Modeling of the kinematic viscosity of unsaturated FAMES, using ANFIS

Figure 5.8: Reveals a perfect illustration of the results of fitting the predicted and experimental values for the kinematic viscosity of unsaturated fatty acid methyl biodiesel. From the nature of the graph, it can be publicized that these values are closed to unity. This greatly highlights an appropriate fitting of the predicted values by the adopted methodology. Table 5.5.3: Shows some contrast between the predicted and experimental values. Virtually from the table, the ANFIS results deviate very slightly from the experimental results. Furthermore the absolute error R^2 is 0.962. This gives an admirable harmony between the experimental and predicted values

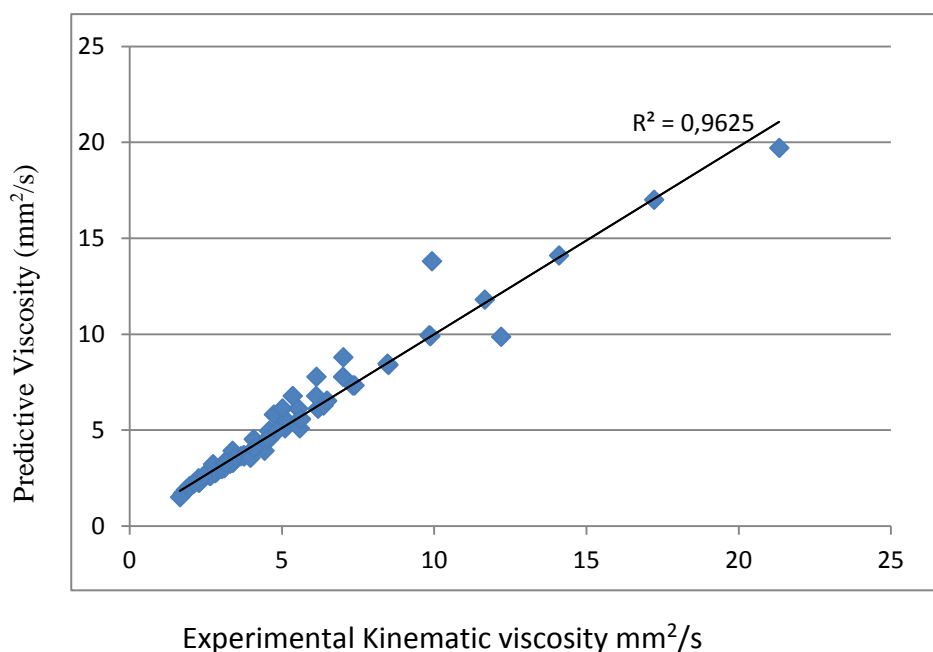


Figure 5.8: Plot of experimental values versus ANFIS values for unsaturated kinematic viscosity of FAME.

Table 5.10: Comparative study between experimental and ANFIS results of unsaturated fatty acid methyl biodiesel.

T (K)	NC	NH	Kinematic Viscosity		Absolute
			(mm²/s)		Error
			EXP	ANFIS	(%)
313.15	19	36	4.573	4.52	1.16
303.15	19	32	4.099	4.04	1.44
283.15	19	32	6.177	6.12	0.92
313.15	19	32	3.298	3.27	0.85
273.15	19	34	9.84	9.95	1.12
283.15	19	32	6.176	6.12	0.91
293.15	19	36	7.33	7.33	0
278.15	19	36	11.66	11.8	1.2
263.15	19	34	14.1	14.1	0
278.15	15	28	7.002	7.78	11.11
283.15	19	32	5.53	6.12	10.67
298.15	19	32	4.5011	4.52	0.2
293.15	19	34	5.6194	5.58	0.7
333.15	19	34	2.644	2.64	0.15
318.15	19	36	4.123	4.05	1.77
273.15	15	28	7.01	8.8	2.53
308.15	19	36	5.099	5.09	0.18
288.15	19	32	5.5241	5.49	0.62
343.15	19	36	2.651	2.63	0.79
358.15	19	32	1.742	1.71	1.26
353.15	19	32	1.845	1.89	2.44

Table 5.1: Continued

T (K)	NC	NH	Kinematic Viscosity (mm²/s)		Absolute Error (%)
			EXP	ANFIS	
293.15	19	36	7.38	7.32	0.81
318.15	15	28	2.85	2.92	2.46
283.15	15	28	6.122	6.78	10.75
343.15	19	32	2.1	2.22	5.71
338.15	19	36	2.871	2.86	0.38
308.15	19	32	3.7504	3.62	3.48
343.15	19	34	2.283	2.27	0.57
333.15	19	36	3.121	3.14	0.61
318.15	19	36	4.125	4.05	1.81
313.15	19	32	3.14	3.27	4.14
343.15	19	34	2.2832	2.27	0.58
313.15	19	32	3.298	3.27	0.85
288.15	15	28	4.73	5.81	22.8
303.15	15	28	4.42	3.93	11.09
318.15	19	32	3.028	2.98	1.62
323.15	19	34	3.103	3.03	2.35
348.15	19	32	1.9598	2.06	5.11
323.15	19	34	3.103	3.03	2.35
288.15	19	32	5.524	5.49	0.62
303.15	19	34	4.53	4.53	0
283.15	19	36	9.869	9.9	0.31
318.15	19	34	3.3826	3.3	2.44
283.15	15	28	5.35	6.78	26.73
293.15	19	32	4.57	4.95	8.32
323.15	19	32	2.8109	2.76	1.81

Table 5.1: Continued

T			Kinematic Viscosity		Absolute
			(mm ² /s)		Error
			(K)	NC	NH
353.15	19	32	1.8455	1.89	2.41
313.15	15	28	2.73	3.22	17.95
288.15	19	34	6.355	6.28	1.18
318.15	19	34	3.103	3.3	2.35
278.15	15	28	6.13	7.78	26.92
333.15	19	32	2.263	2.49	10.03
298.15	19	36	6.472	6.52	0.74
293.15	19	32	4.84	4.95	2.27
313.15	19	32	3.298	3.27	0.85
353.15	19	34	1.966	2.03	3.26
263.15	15	28	9.92	13.8	39.11
278.15	19	34	8.46	8.46	0
323.15	19	36	3.741	3.69	1.36
343.15	19	34	2.25	2.27	0.89
323.15	19	36	3.742	3.69	1.39
328.15	19	32	2.629	2.6	1.1
308.15	15	28	3.432	3.56	3.73
289.15	19	34	5.017	6.12	21.99
313.15	19	32	3.298	3.27	0.85
293.15	19	34	5.58	5.09	8.78
308.15	15	28	3.96	3.56	10.1
363.15	19	32	1.649	1.51	8.43
348.15	19	32	1.9621	2.06	4.99

Table 5.1: Continued

T (K)	NC	NH	Kinematic Viscosity		Absolute
			(mm ² /s)		Error
			EXP	ANFIS	(%)
268.15	19	36	17.22	17	1.28
263.15	19	36	21.33	19.7	7.64
308.15	19	34	4.075	4.05	0.61
303.15	19	34	4.5079	4.53	0.49
313.15	19	32	3.14	3.27	4

5.5 Response Surface Methodology Model for kinematic Viscosity of Saturated Fatty Acid Methyl esters

Influence of temperature, number of carbon atoms, and number of hydrogen atoms on the viscosity of saturated fatty acid methyl biodiesel was tested with RSM. The experimental runs were randomly done, to minimize the effect of unexpected variability in the observed responses. The adopted methodology allowed the formation of a quadratic equation. The three parameters used were represented in the quadratic equation as shown

$$\nu = 2.3439 - 1.1942x_1 + 1.5018x_3 + 0.3374x_1^2 + 0.1971x_2^2 - 0.6816x_1 * x_2 \quad (5.1)$$

Where x_1 is T, the temperature in Kelvin (K)

x_2 is NC, the number of Carbon Atoms

x_3 is NH, the number of Hydrogen Atoms

Experimental data values from literature search were substituted in the quadratic equation above to predict kinematic viscosity values for RSM. The results are summarized in the Table 5.11, on page 69.

The predictive ability of the equation is measured with the use of R^2 . Due to the interactive effects between the variables, the parameters cannot be analyzed independently. The significance of the parameters in the model was obtained using Minitab, using regression. The contour plots and surface view (3D) are shown in Figures 5.9 and 5.10 underneath.

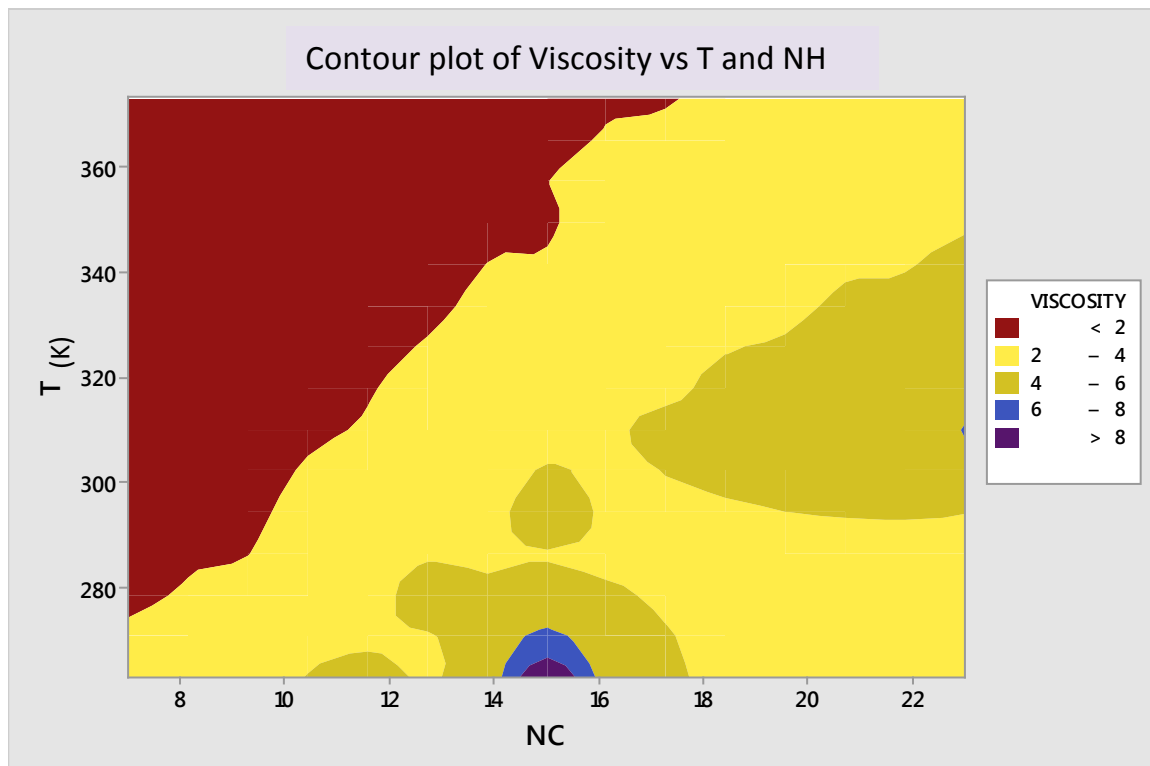


Figure 5.9: Contour plot for saturated kinematic viscosity, using RSM prediction model, with NC as parameter.

This plot helps to explain how the kinematic viscosity of saturated fatty acid methyl biodiesel varies with temperature and number of carbon atoms in the fatty acid. Most significantly, the contour plots are useful tools for identifying the optimum operating conditions and related response value. The points on each contour indicate the kinematic viscosity of the FAME biodiesel, in the specified temperature and number of carbon atoms.

If the plotting parameters or variables are changed, the contour plots changes. The figure below shows another contour plot of viscosity, temperature and number of hydrogen atoms.

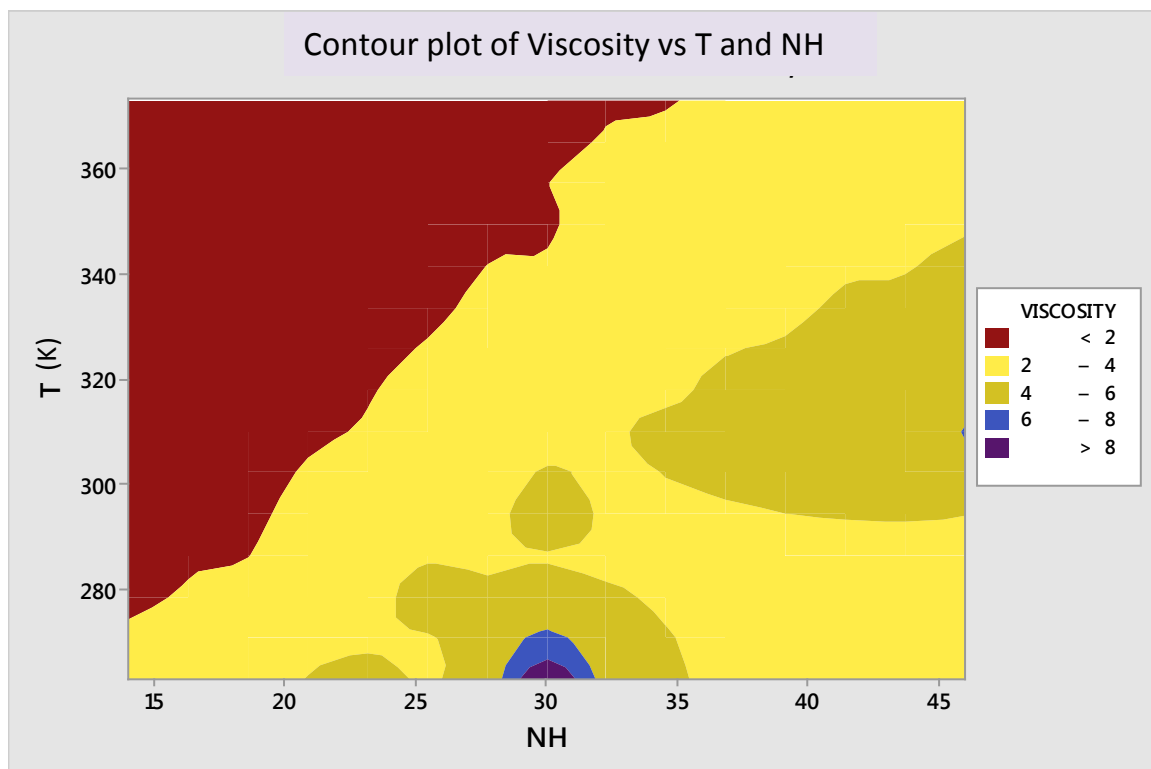


Figure 5.10: Contour plot of kinematic viscosity for saturated with NH, as parameter

In a similar manner, the surface plot is a 3D plot involving the viscosity, temperature, and number of carbon atoms. The points on the surface plot equally indicate the kinematic viscosity.

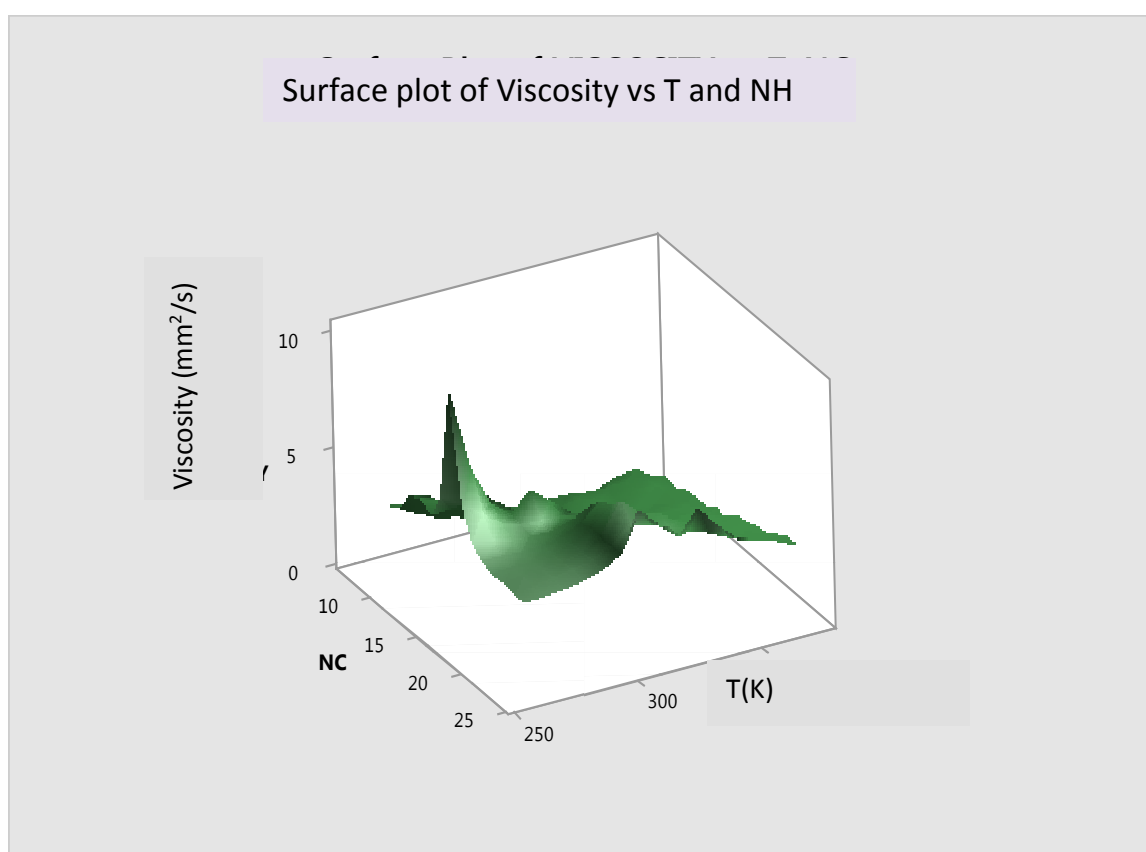


Figure 5.11: Surface plot of viscosity versus temperature and number of carbon atoms

If the plotting parameters are changed, the shape of the surface plots changes. This can be illustrated in the 3D arrangement below, which involve the temperature, viscosity and the number of hydrogen atoms as parameters

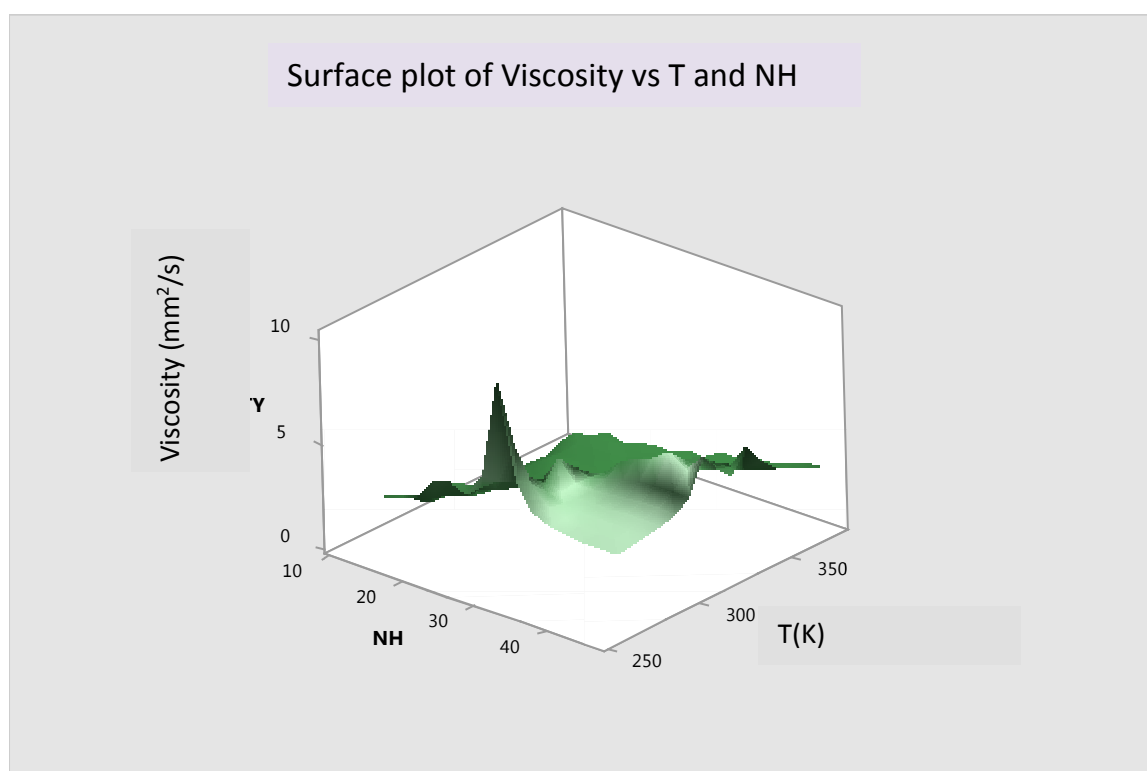


Figure 5.12: Surface plot structure for viscosity versus temperature and number of hydrogen atoms

The difference between the actual data and predicted data of the kinematic viscosity of saturated fatty acid methyl biodiesel indicates the residual. A plot of residual versus fitted values for saturated FAMES is shown below

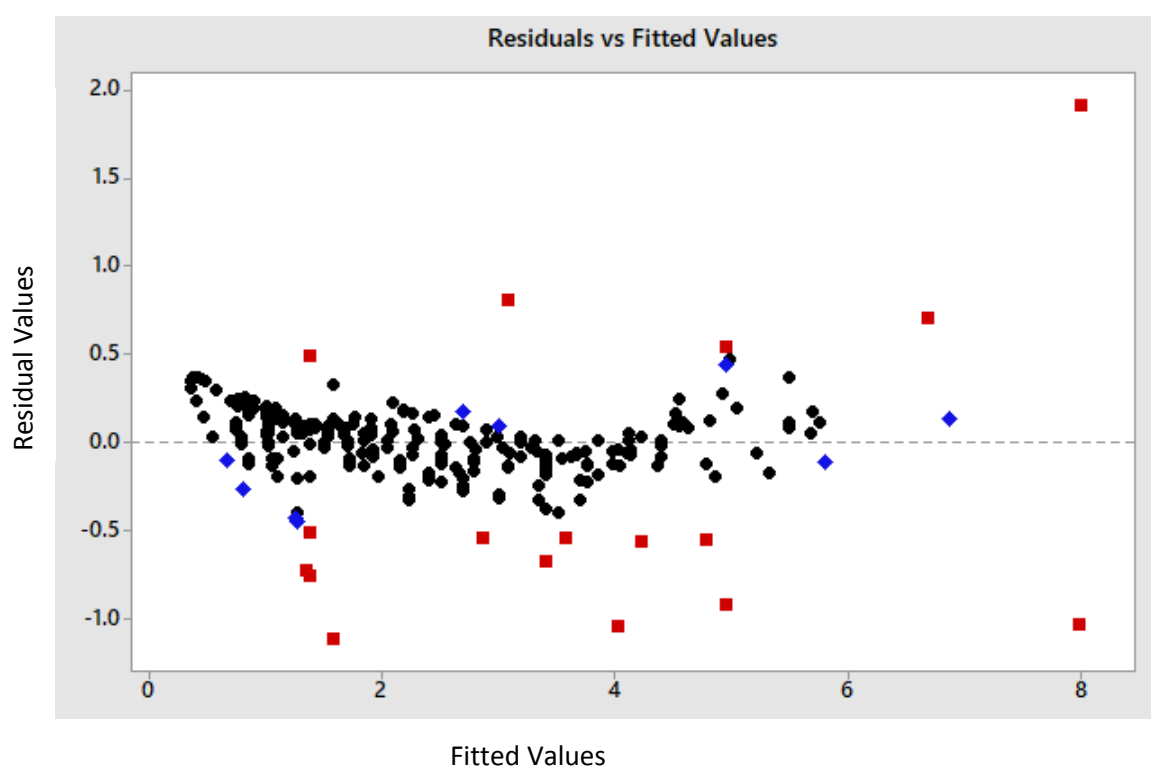
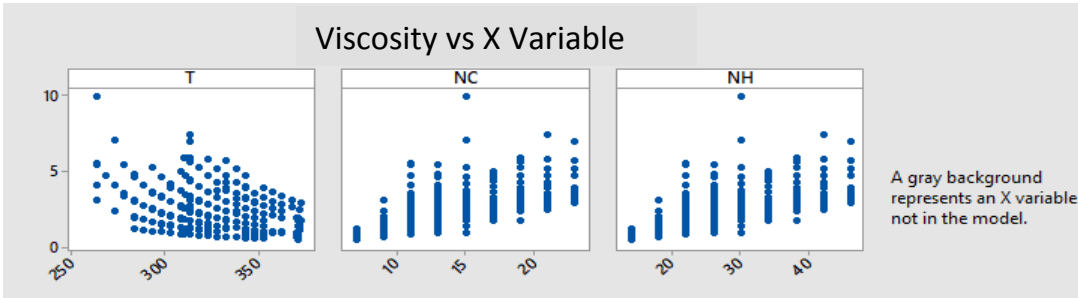
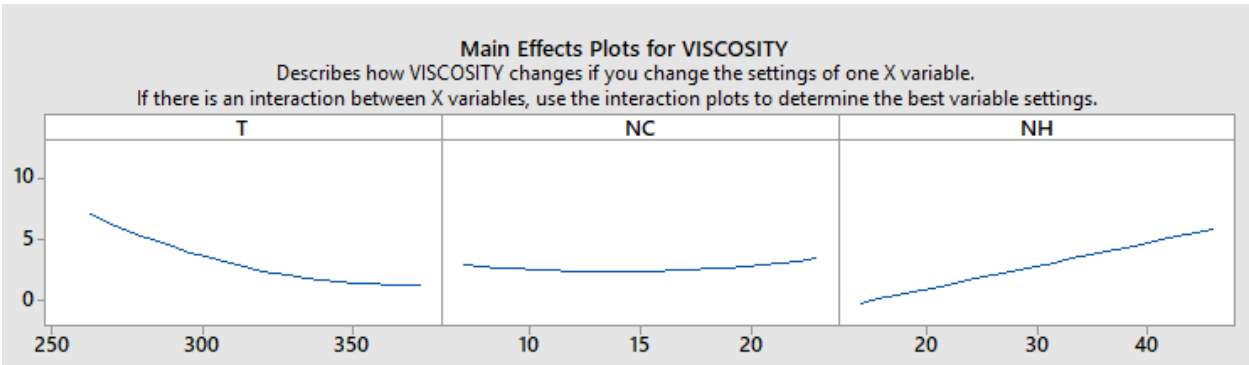


Figure 5.13: Plot of residual values versus fitted values, for saturated FAME

Plots of viscosity versus the different variables used in this model are shown below. This consist plotting viscosity against temperature, number of carbon atoms and number of hydrogen atoms, on different axes



When the setting of variables is changed, viscosity changes. This is illustrated in the curves below.



Figures 5.14: Plots of viscosity with a single parameter

5.6. Response Surface Methodology for the Kinematic Viscosity of Unsaturated Fatty Acid Methyl Biodiesel

Influence of temperature, number of carbon atoms, and number of hydrogen atoms on the viscosity of unsaturated fatty acid methyl biodiesel was tested with RSM. The experimental runs were randomly done, to minimize the effect of unexpected variability in the observed responses. The adopted methodology allowed the formation of a quadratic equation. The three parameters used were represented in the quadratic equation as shown.

$$\text{Viscosity} = 263.3 - 1.0861x_1 - 3.271x_2 - 3.147x_3 + 0.001845x_1^2 + 0.1067x_3^2 + 0.01121x_1 * x_2 + 0.01134x_1 * x_3 \quad (5.2)$$

Where x_1 is T, the temperature in Kelvin

x_2 is NC, the number of Carbon atoms

x_3 is NH, the number of hydrogen atoms

Experimental data values from literature search were substituted in the quadratic equation above to predict kinematic viscosity values for RSM. The results are summarized in the table

The predictive ability of the equation is measured with the use of R^2 . Due to the interactive effects between the variables, the parameters cannot be analyzed independently. The significance of the parameters in the model was obtained with the aid of Minitab application, using regression. The contour plots and surface view (3D) are shown below.

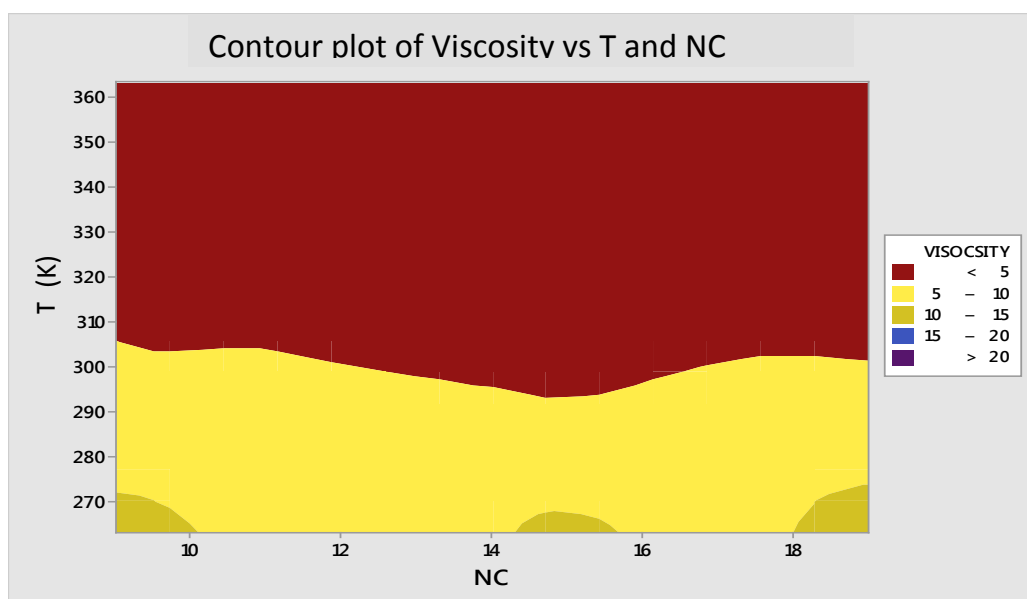


Figure 5.15: Contour plot for viscosity versus T, NC, for unsaturated FAME

This plot helps to explain how the kinematic viscosity of unsaturated fatty acid methyl biodiesel varies with temperature and number of carbon atoms in the fatty acid. Most significantly, the contour plots are useful tools for identifying the optimum operating conditions and related response value. The points on each contour indicate the kinematic viscosity of the unsaturated FAME biodiesel, in the specified temperature and number of carbon atoms

If the plotting parameters or variables are changed, the contour plots changes. The figure below shows another contour plot of viscosity, temperature and number of hydrogen atoms as parameters

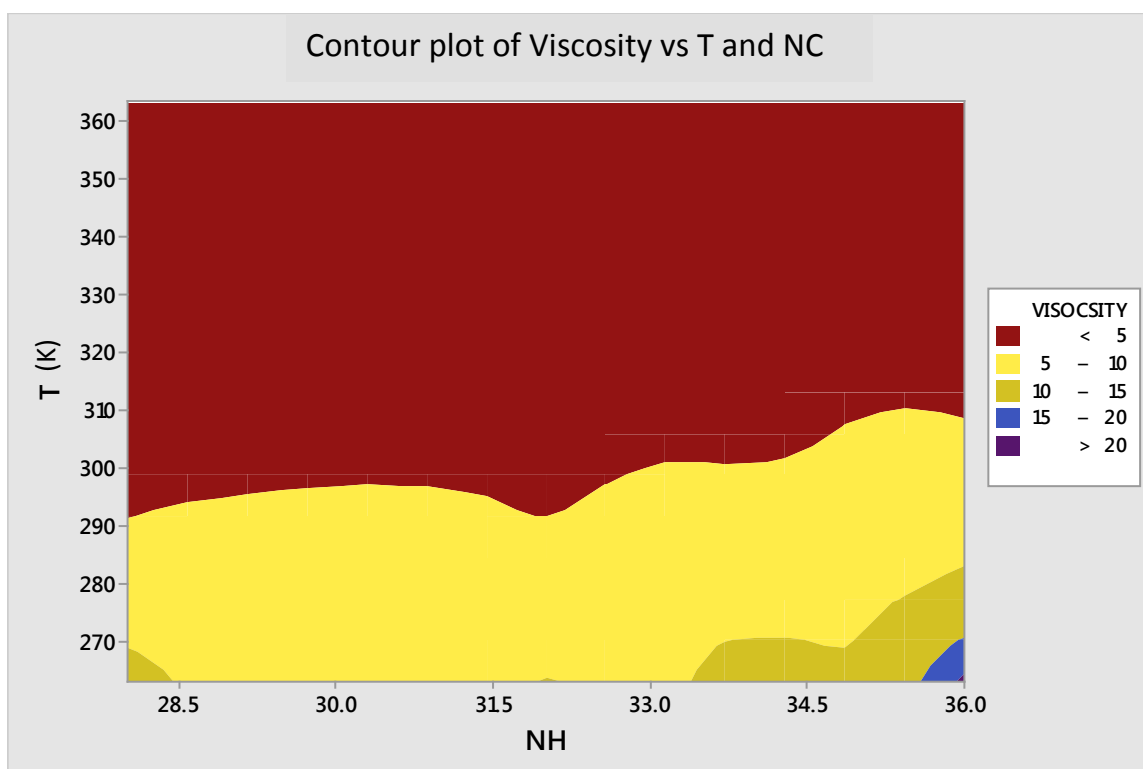


Figure 5.16: Contour plot for viscosity versus T, NH for unsaturated FAME

In a similar manner, the surface plot is a 3D plot involving the viscosity, temperature, and number of carbon atoms. The points on the surface plot equally indicate the kinematic viscosity.

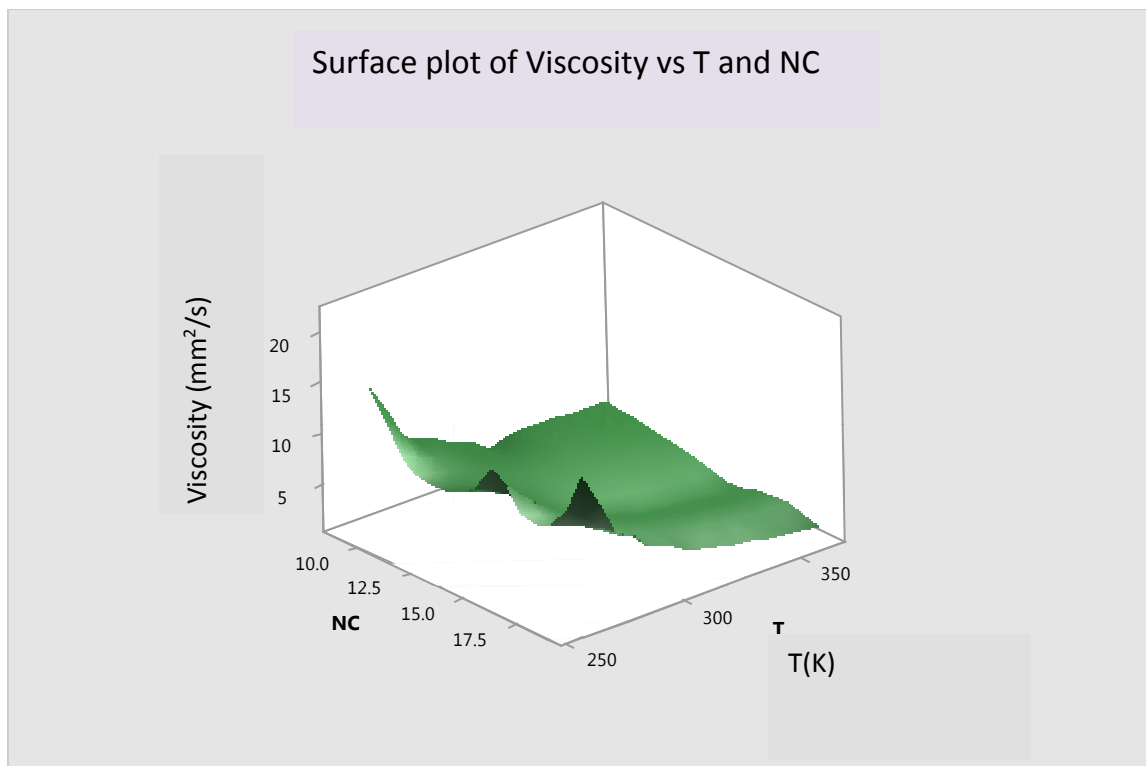


Figure 5.17: Surface plot for viscosity versus T, NC, for unsaturated FAME

If the plotting parameters are changed, the shape of the surface plots changes. This can be illustrated in the 3D arrangement below, which involve the temperature, viscosity and the number of hydrogen atoms as parameters

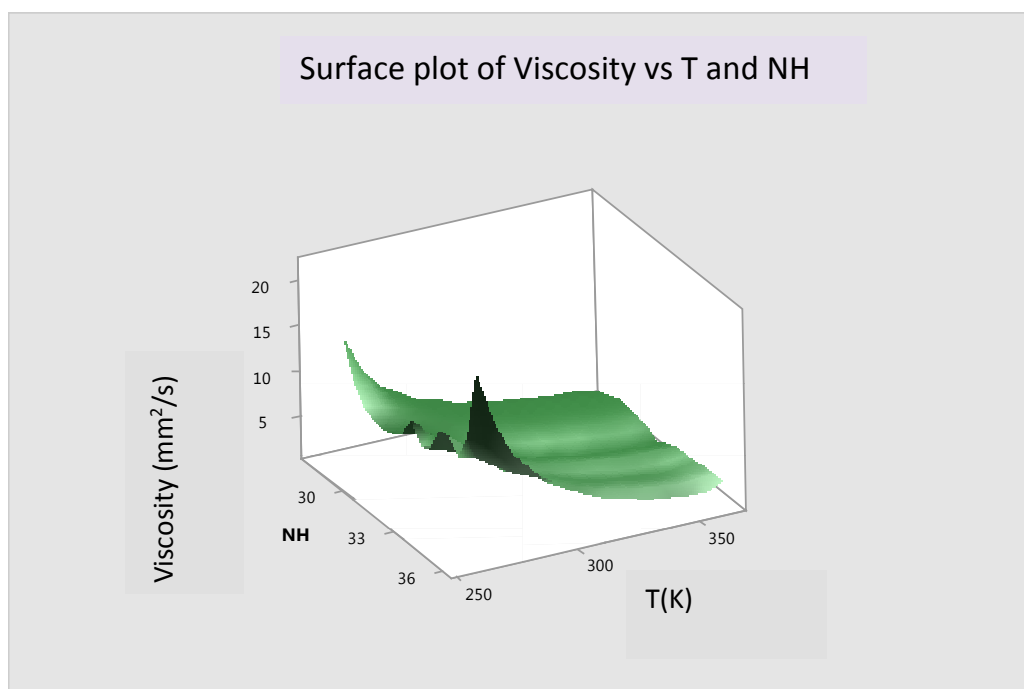


Figure 5.18: Contour plot of viscosity versus T , NH for unsaturated FAME.

Plots of viscosity versus the different variables used in this model are shown below. This consist plotting viscosity against temperature, number of carbon atoms and number of hydrogen atoms, on different axes

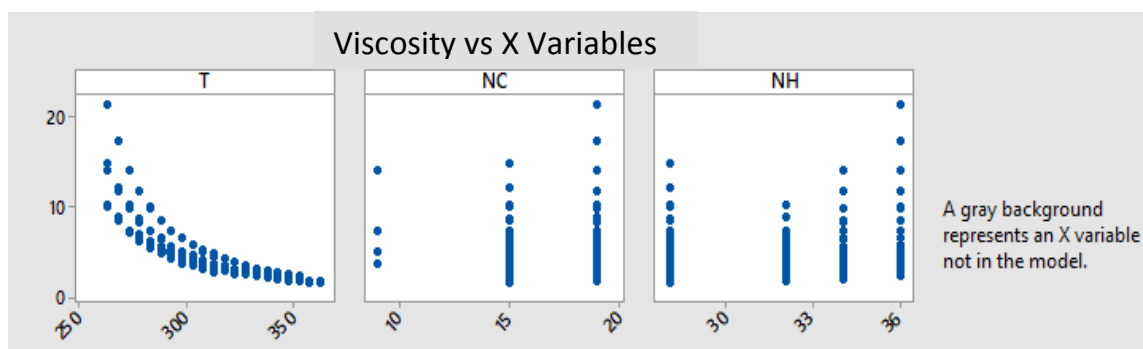


Figure 5.19: Plots of viscosity versus single variable, for unsaturated FAME

As the setting of variables change the viscosity changes. This is illustrated in the curves below

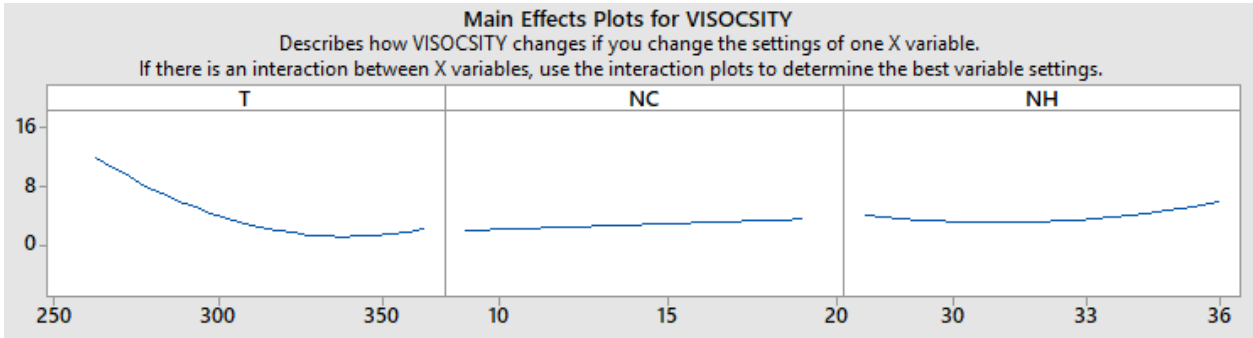


Figure 5.20: Viscosity changes with different parameter plots, for unsaturated FAME

The residual indicates the difference between the predicted data and the actual data of kinematic viscosity of unsaturated fatty methyl acid biodiesel.

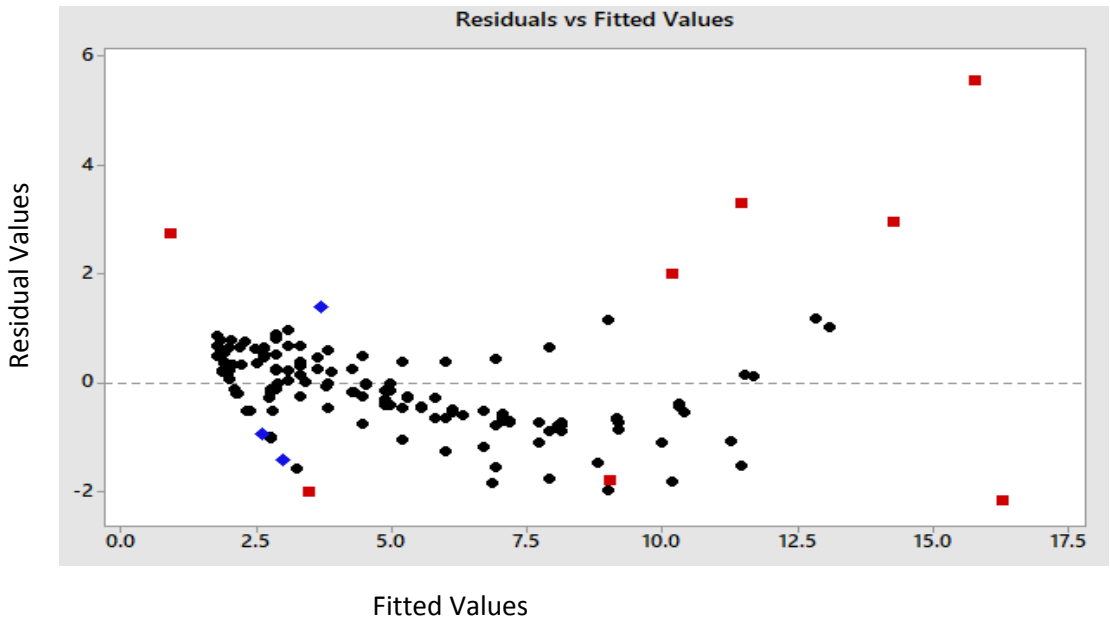


Figure 5.21: Plot of residual versus fitted values

5.7. Summary of the Response Surface methodology Results (RSM)

The input data in the Minitab 17 software led to the formation of mathematical equations for both the saturated and unsaturated fatty acid methyl biodiesel kinematic viscosities. With several constant coefficients x_1 , x_2 and x_3 attached to the parameters. Where, x_1 is the temperature, x_2 is the number of carbon atoms and x_2 is the number of hydrogen atoms. This is illustrated in the table below.

Table 5.11: RSM results for saturated and unsaturated FAME

Equation	Coefficient							System	R^2
4.1	1.1942	1.5018	0.3374	0.1971	0.6816			Saturated	0.97
4.2	1.0861	3.271	3.147	0.001845	0.1067	0.01121	0.01134	Unsaturated	0.96

5.8. Mathematical Model

The mathematical equations 1.4 and 1.5 were used to predict the kinematic viscosity of saturated and unsaturated fatty acid methyl biodiesel. The development of the proposed model involved the modeling of expressions reported in the literature review, in which parameters A, B, C, D, are obtained and substituted in the above equations, to predict the kinematic viscosity. Some of the results are summarized in the table below.

Table 5.12: Mathematical model results for saturated FAME

Temp (k)	NC	NH	EXP viscosity	A	B	C	D	Predicted viscosity
273.15	15	30	7.01	-3.43	-0.087	796.62	69.966	7.565
293.15	13	26	3.641	-3.43	-0.087	796.62	69.966	3.522
293.15	13	26	3.627	-3.43	-0.087	796.62	69.966	3.522
358.15	19	38	2.54	-3.43	-0.087	796.62	69.966	2.347
298.15	13	26	3.29	-3.43	-0.087	796.62	69.966	3.195
313.15	13	26	2.4331	-3.43	-0.087	796.62	69.966	2.429
283.15	11	22	3.1	-3.43	-0.087	796.62	69.966	3.141
293.15	11	22	2.4331	-3.43	-0.087	796.62	69.966	2.601
313.15	15	30	3.3	-3.43	-0.087	796.62	69.966	3.121
333.15	13	26	1.732	-3.43	-0.087	796.62	69.966	1.751
338.15	23	46	5.143	-3.43	-0.087	796.62	69.966	5.385
363.15	17	34	1.905	-3.43	-0.087	796.62	69.966	1.751
283.15	9	18	1.913	-3.43	-0.087	796.62	69.966	2.280
318.15	11	22	1.598	-3.43	-0.087	796.62	69.966	1.709
313.15	11	22	1.726	-3.43	-0.087	796.62	69.966	1.847

The figure below shows the comparisons of mathematical predicted results and experimental data. The R^2 value shown is closed to unity, articulating the proper fitting of predicted values and experimental data

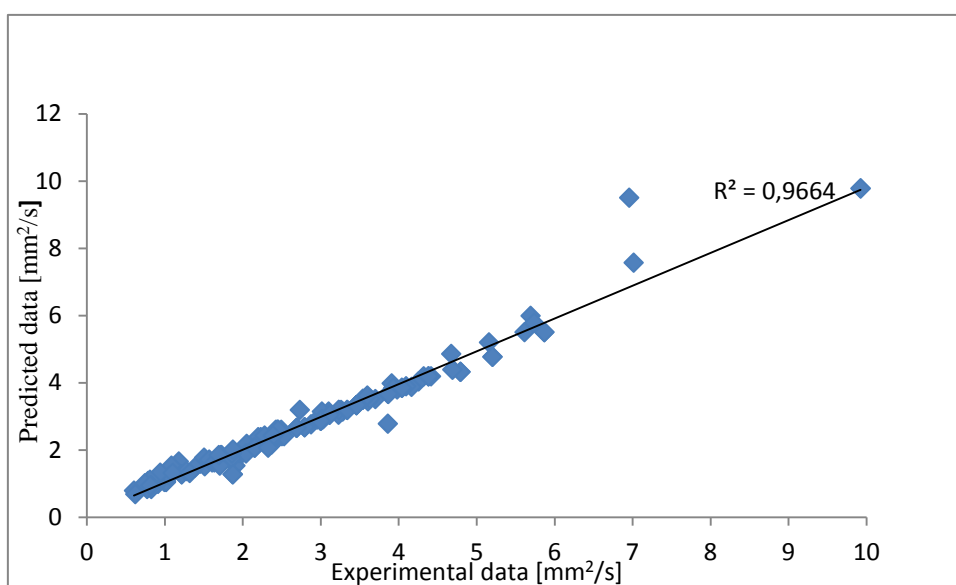


Figure 5.22: Fitting of predicted kinematic viscosity values for saturated FAME, and experimental values.

Table 5.13: Mathematical prediction of unsaturated kinematic viscosity for FAME s

Temp (K)	NC	NH	EXPA	A	B	C	D	Viscosity mm²/s
313.15	19	36	4.573	-9.228	0.181	3020.014	-47.957	3.704
303.15	19	32	4.099	-9.288	0.181	3020.014	-47.957	4.681
283.15	19	32	6.177	-9.288	0.181	3020.014	-47.957	7.857
293.15	19	32	3.298	-9.288	0.181	3020.014	-47.957	3.704
273.15	19	32	9.84	-9.288	0.181	3020.014	-47.957	10.473
283.15	19	34	6.176	-9.288	0.181	3020.014	-47.957	7.857
293.15	19	36	7.33	-9.288	0.181	3020.014	-47.957	6.011
278.15	15	36	11.66	-9.288	0.181	3020.014	-47.957	9.047
263.15	19	34	14.1	-9.288	0.181	3020.014	-47.957	14.268
278.15	15	36	7.002	-9.288	0.181	3020.014	-47.957	8.019
283.15	19	32	5.53	-9.288	0.181	3020.014	-47.957	7.857
298.15	19	32	4.5011	-9.288	0.181	3020.014	-57.957	5.293
293.15	19	34	5.6194	-9.288	0.181	3020.014	-57.957	6.011
333.15	19	34	2.644	-9.288	0.181	3020.014	-57.957	2.419
318.15	19	36	4.123	-9.288	0.181	3020.014	-57.957	3.313
288.15	19	32	7.011	-9.288	0.181	3020.014	-47.957	6.856
268.15	15	28	5.099	-9.288	0.181	3020.014	-47.957	1.991
308.15	19	36	5.5241	-9.288	0.181	3020.014	-41.957	5.099
343.15	19	34	2.651	-9.288	0.181	3020.014	-41.957	1.991

The fitting of the predicted kinematic viscosity values of unsaturated FAME, using the mathematical model were slightly not very closed to unity as those of the saturated fatty acid FAME biodiesel. Notably the R^2 value of the unsaturated FAME is small that of saturated FAME. This can be illustrated in the graph below.

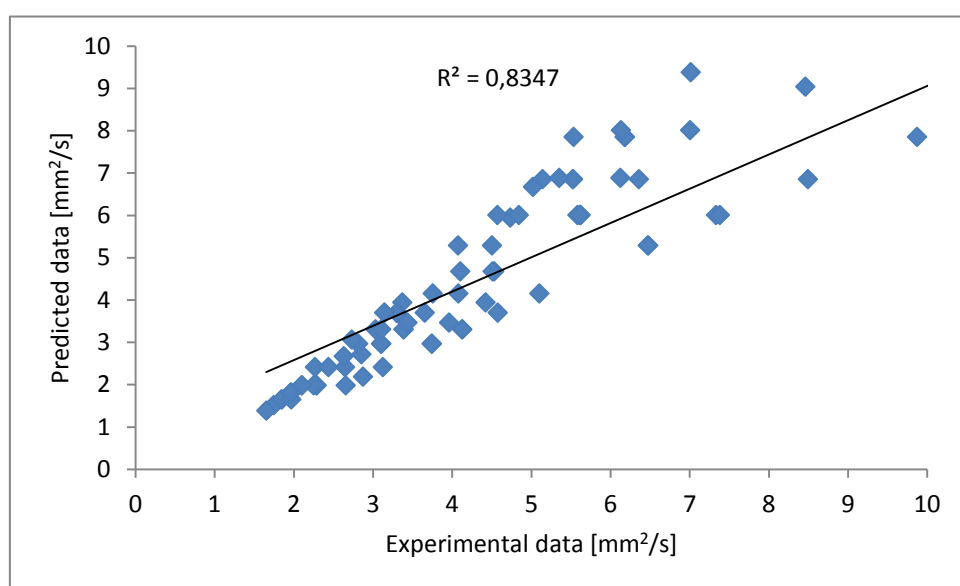


Figure 5.23: Fitting of predicted kinematic viscosity values of unsaturated FAME, with experimental values, for the mathematical model.

5.9. Comparing the correlation models for FAMEs biodiesel

The three correlation models used in this work are compared in the table below

Table 5.14: R^2 values for the various models

Correlation Model	System Type	R^2 Value
ANFIS	Saturated	0.976
RSM		0.97
Mathematical Model		0.966
ANFIS	Unsaturated	0.962
RSM		0.96
Mathematical Model		0.834

CHAPTER 6

CONCLUSIONS

Considering its significance in engine performance, viscosity is regarded an important property of biodiesel. As a matter of fact, unfailing mathematical models that can precisely measure kinematic viscosity as a function of temperature are crucial for the improvement of combustion models and the design of process machineries.

The Response Surface Methodology approach generated two mathematical equations, alongside coefficients, based on the input data of temperature, number of hydrogen atoms and number of carbon atoms of the FAMES that were used to predict kinematic viscosity.

Generally three empirical models were engaged, the ANFIS, RSM, and Mathematical correlation, to predict the kinematic viscosity of fatty acid methyl biodiesel. Each of the models was discretely used to predict the kinematic viscosity of saturated and unsaturated methyl fatty acid ester biodiesel. The predicted results from the three models were compared with the experimental results from the literature review and resulted to the following conclusions

- Kinematic viscosity values for unsaturated fatty acid methyl esters biodiesel are higher than those of saturated fatty acid methyl esters biodiesel.
- FAMES kinematic viscosity decreases with increasing temperature.
- There is a brilliant agreement between the experimental data and predicted data for the kinematic viscosity of FAME biodiesel.
- R^2 for ANFIS was near to unity, especially for saturated FAMES, with value 0.976.

Therefore the ANFIS model is better than RSM and Mathematical model used in this work.

Owing the importance of biodiesel as a remedy to the energy crisis in the world today, a lot is left undone in this field of research. Other properties of biodiesel, like specific density, flash point etc, can be studied in order to improve system performance.

Similarly, the variation of quality of biodiesel blends with changes in temperature is of paramount importance.

REFERENCES

- Amin, A., Gadallah, A., El Morsi, A., El-Ibiari, N., & El-Diwani, G. (2016). Experimental and empirical study of diesel and castor biodiesel blending effect, on kinematic viscosity, density and caloric value. *Egyptian Journal of Petroleum*, 25(4), 509-514.
- Bonhorst, C. W., Althouse, P. M., Triebold, H. (1948). Esters of naturally occurring fatty acids. Physical properties of methyl, propyl, and isopropyl esters of C6–C18 saturated fatty acids. *Ind Eng chem*; 40 (12), 2379–2385.
- Canon, M. R., and Manning, R. E. (1960). “Viscosity measurement” Analytical chemistry. *ANCHA*, 32(5), 355-357.
- Canon, M. R., and Fenske, M. R. (1941). “Viscosity measurement-Opaque liquids industrial and engineering chemistry, Analytical Edition. *ANCHA*, 13(3), 299-300
- Canon, M. R., and Fenske, M. R. (1938) “Viscosity measurement “ industrial and engineering chemistry. Analytical Edition. *ANCHA*, 10 (3), 297-298.
- Castilo, O., and Melin, P. (2008) Type-2 fuzzy logic: Theory and application. *Springer*, 78(6), 67-82
- Docarmo, F., Sousa, P. M., Santiago-Aguiar, R. S. (2012). Development of a new model for biodiesel viscosity prediction based on the principle of corresponding state. *Fuel*, 92(1), 250–257.
- Felipe, R. (2012). Density and viscosity of biodiesel as a function of temperature. Empirical model. *Renewable and sustainable energy review*, 19(2), 652-665
- Fritz Simons, O. (1935). “A Rapid Precision Viscometer” industrial and engineering chemistry, Analytical edition. *ANCHA*, 7(2), 193-198.

- Gerhard, K., Kevin, R., and Steidley, P. (2001). Kinematic viscosity of biodiesel components (fatty acid alkyl esters). *Fuels*, 98(6), 122-125
- Gerhard, K., Kevin, R. (2014). A Comprehensive Evaluation of the Density of Neat Fatty Acid. *Fuels*, 34(5), 154-163
- Gouw, T., Vuggter, J. C., Roelands. (1966). Physical properties of fatty acid methyl esters. *Chem Soc* , 43 (7), 433-434.
- Jang, R. J, & Sun, C. T. (1995) . Neuro-fuzzy modeling and control. *proc IEEE*, 83(4), 378-404.
- Juan, C., Chavarria-Hernandez, Daniella, E. and Pacheco-Catalán. (2013). Predicting the kinematic viscosity of FAMEs and biodiesel. *Fuels*,80(3), 23-32.
- Knothe, G., Steidley, K. R. (2007). Kinematic viscosity of biodiesel components (fatty acid alkyl esters) and related compounds at low temperature. *Fuel*, 86(16), 26-29.
- K. Y., Liew, C. E., Seng and L. Oh. (2006). Viscosities and Densities of the Methyl Esters of Some n-Alkanoic Acids. An empirical approach in predicting biodiesel viscosity at various temperatures. *Fuel*, 85(1), 107–113.
- L. Meher, D., Vidya, S. (2006). Technical aspects of biodiesel production by Trans esterification - a review. *Renewable and sustainable energy reviews*, 10(2), 20-26.
- Lapuerta, M., Rodriguez-Fernandez, J., Armas, O. (2010). Correlation for the estimation of the density of fatty acid esters fuels and its implications. A proposed biodiesel. *cetaneindex.Chemistry and Physics of Lipids* , 63(7), 20-28.
- Liew, K. Y., Seng, C. E., Oh, I. L. (1992). Viscosity and density of the methyl esters of some n-alkanoic acids. *J Am Oil Chem Soc*, 69(2), 155-158.
- Maria, J., Pratas, S., Freitas, M., Oliveira, S. C., Monteiro, A. S., Lima, A. and Joa.,P. Coutinho. (2010). Densities and Viscosities of Fatty Acid Methyl and Ethyl Esters. *Chem data*, 55(7), 3983–3990.

- Nelles, O. (2001). Nonlinear system identification: From classical approaches to neural Networks and fuzzy Design and Analysis of Experiments, Response surface Method and designs. *A comprehensive foundation*, 91(1), 35-40
- Nogueira, C. A., Feitosa, F.X., Fernandes FAN, Santiago, R. S.(2010). Density and Viscosity of binary mixtures of babassu biodiesel + cotton seed or soya beans at different temperatures. *Journal of Chemical and engineering data*, 55(7),21-29.
- Pratas, M. J., Freitas, S., Oliveira, M. B., Monteiro, S. C., Lima, A. S. and Coutinho, J. (2010). Densities and Viscosities of fatty acid methyl and ethyl esters. *Journal of Chemical and Engineering Data*, 55(4), 83–90.
- Pratas, M. J., Freitas, S., Oliveira, M. B., Monteiro, S.C. and Lima, A. S. (2011). Biodiesel density: experimental measurements and prediction models. *Energy Fuel*, 25(2), 33–40.
- Ramírez, L. F. (2013). Density and viscosity of biodiesel as a function of temperature. Empirical models. *Renew Sustain Energy* 19(6), 52–65.
- Robert, C. (2013). The Properties of Gases and Liquids. Empirical models. *Renew Sustain Energy*, 19(6), 52–56.
- Suriya, P., Kaokanya, S., Supathra, L., Kornkanok A. and Kanit, K. (2015). An Empirical Equation for Estimation of Kinematic Viscosity of Fatty Acid Methyl Esters and Biodiesel. *Fuels*, 15(26), 67-69.
- Sugeno, M. & Kang, G. T. (1988). Structure identification of Fuzzy model, *fuzzy set syst*, 28 (1), 15-33.
- Shu, Q., Yang, B., Yang, J., Qing, S. (2007). Predicting the viscosity of biodiesel fuels based on the mixture topological index method. *Fuel*, 86(18), 49–54.
- Tushar, K. and Dasika, H. (2007). Viscosity of Liquids. Theory, Estimation, Experiment, and Data. *Springer*, 34 (3), 46-48

- Takagi, T. & Sugeno, M. (1985). Fuzzy identification of systems and its applications to modeling and control, *IEEE Trans system and Man Cybernet*, 15(1), 116-132.
- Tsukamoto, Y., Gupta, M. M., Ragade, R. K., & Yager, R. R. (1979). ‘‘An approach to fuzzy reasoning method’’, in *Advances in Fuzzy Set Theory and Application. Fuel*, 13(7), 44-49.
- V. Ogel, H. (1992). The law of the relation between the viscosity of liquids and the temperature. *Phys z*, 22(6), 45-69.
- Yuan, W., Hansen, A. C., Zhang, Q. (2009). Predicting the temperature dependent viscosity of biodiesel *fuels*. *Fuel*, 88(11), 20–26.